

Deep Controlled Learning for Inventory Control

Tarkan Temizöz, Christina Imdahl, Remco Dijkman,
Douniel Lamghari-Idrissi, Willem van Jaarsveld
Eindhoven University of Technology

Abstract

Problem definition: Are traditional deep reinforcement learning (DRL) algorithms, developed for a broad range of purposes including game-play and robotics, the most suitable machine learning algorithms for applications in inventory control? To what extent would DRL algorithms tailored to the unique characteristics of inventory control problems provide superior performance compared to DRL and traditional benchmarks? **Methodology/results:** We propose and study Deep Controlled Learning (DCL), a new DRL framework based on approximate policy iteration specifically designed to tackle inventory problems. Comparative evaluations reveal that DCL outperforms existing state-of-the-art heuristics in lost sales inventory control, perishable inventory systems, and inventory systems with random lead times, achieving lower average costs across all test instances and maintaining an optimality gap of no more than 0.1%. Notably, the same hyperparameter set is utilized across all experiments, underscoring the robustness and generalizability of the proposed method. **Managerial implications:** These substantial performance and robustness improvements pave the way for the effective application of tailored DRL algorithms to inventory management problems, empowering decision-makers to optimize stock levels, minimize costs, and enhance responsiveness across various industries.

Keywords: inventory theory and control, OM-information technology interface, lost sales, deep reinforcement learning.

1 Introduction

Inventory management problems play a critical role in supply chain and logistics as they directly influence a company’s financial performance (Silver et al., 1998). The field encompasses a diverse array of challenges, such as mitigating lost sales due to stockouts (e.g., Bijvank and Vis, 2011), managing products with limited shelf life (e.g., Karaesmen et al., 2011), and inventory control with random replenishment lead times (e.g., Zipkin, 2000). The decision-making process in these systems is intricate due to the high degree of stochasticity resulting from exogenous factors such as demand uncertainty and stochastic lead times. In addition, each of these problems comes with unique operational dynamics, making their solutions substantially distinct from one another. For instance, managing perishable products may necessitate aggressive inventory reduction strategies to minimize waste (Nahmias, 1975a), while navigating uncertain lead times may demand maintaining higher stock levels and robust contingency plans (Zipkin, 2000). As a result, addressing these challenges requires tailored approaches.

Optimal solutions for these problems are often computationally intractable (Federgruen and Zipkin, 1984) due to the exponential growth in possible combinations of states, actions, and uncertain scenarios, resulting from their high dimensionality and stochastic nature. Consequently, researchers frequently resort to approximate methods to model and solve these problems (Zipkin, 2000). In this context, Markov Decision Processes (MDPs) are frequently employed to tackle inventory management problems, as they adeptly capture underlying uncertainties and accommodate sequential decision-making processes. To address the intractability of MDPs, various approximate dynamic programming (ADP) methods have been explored (Powell, 2011). However, these methods often have problem-specific limitations, such as requiring a maximum lead time of one (e.g. Chen et al., 2014), or depend on exploiting cost-structure information, such as the cost function exhibiting L^1 convexity (e.g. Sun et al., 2016). However, as Cachon et al. (2020) notes, achieving more impactful inventory management requires more broadly applicable approaches.

Deep reinforcement learning (DRL) offers a promising alternative by integrating neural networks with reinforcement learning, enabling the learning of complex decision-making processes in high-dimensional state spaces (Mnih et al., 2015). DRL algorithms utilize neural networks to approximate the relationship between system states and decisions, iteratively refining the decision-making process. By leveraging the power of neural networks, DRL has the potential to overcome some limitations of traditional methods, including problem-specific constraints. This is evidenced by its empirical success as a general-purpose algorithm across a wide range of applications, including Atari games (Mnih et al., 2015) and board games (Silver et al., 2018). Building on these successes, DRL has been applied to inventory management problems, achieving results comparable to heuristic policies (Gijsbrechts et al., 2022; Oroojlooyjadid et al., 2021; Vanvuchelen et al., 2020).

Despite their successes, DRL algorithms employed in prior studies, such as Asynchronous Advantage Actor-Critic (A3C) (Mnih et al., 2016), Deep Q-Learning (DQN) (Mnih et al., 2015), and Proximal Policy Optimization (Schulman et al., 2017), are not explicitly designed to handle the high level of stochasticity (Trimponias and Dietterich, 2023) particularly inherent in the MDPs commonly encountered in inventory management problems. As highlighted by Powell (2020), such MDPs, also known as Input-Driven MDPs (Mao et al., 2019) or MDPs with exogenous variables (Dietterich et al., 2018), are characterized by an independent stochasticity source exogenous to the MDP that is uncontrollable by decisions. A prime example is *customer demand*, which is independent of replenishment orders in many inventory management applications.

Consequently, these algorithms may not consistently outperform existing state-of-the-art heuristics in inventory management, as evidenced by their performance in the lost sales problem (Gijsbrechts et al., 2022) and perishable inventory systems (De Moor et al., 2022). This limitation can be attributed to several factors that render these algorithms less suitable for addressing such prob-

lems, preventing them from being used in practice. First, algorithms such as A3C and PPO update the policy using trajectories generated by the current policy, which often results in each state being visited a limited number of times. Limited state revisitation and significant variations in trajectory costs, resulting from the high stochasticity of these problems, make it difficult to accurately assess the relative values of actions in a state. Evaluating states under multiple exogenous scenarios is essential to address this issue (Dietterich et al., 2018). However, generating multiple scenarios for state evaluation can be computationally expensive and inefficient, necessitating approaches to address this limitation. Moreover, all three algorithms utilize neural networks to approximate costs tied to policies. In inventory management, stochastic exogenous inputs, such as uncertain demand or lead times, can introduce significant noise into these approximations. This noise can then degrade the accuracy of the estimate of expected trajectory costs, thereby affecting the efficacy of derived policies (see Lazaric et al., 2016, for a similar discussion). In summary, there is a need for DRL algorithms specifically designed to handle these challenges and cater to the unique requirements of inventory management problems.

This paper proposes Deep Controlled Learning (DCL), a new end-to-end DRL framework specifically tailored for inventory management applications. DCL is an approximate policy iteration algorithm that iteratively improves policies by casting reinforcement learning as a classification problem. It employs simulations to collect state-action pairs to form a dataset, which is then used to train neural networks for policy representation. For each state in the dataset, an estimated optimal action is determined by revisiting and evaluating that state under multiple exogenous scenarios and selecting the action with the least estimated expected costs over a trajectory. This estimated action serves as the label for the corresponding state in the classification task, guiding the neural network to map that state to this action. In doing so, DCL iteratively forms datasets and refines policies. Through the strategic use of simulations and careful consideration of various exogenous factors, DCL adeptly addresses the challenges posed by the inherently stochastic nature of inventory management problems.

Furthermore, DCL implements several strategies to reduce the computational burden of simulations and enhance performance. One such strategy is the use of a variance control mechanism called Common Random Numbers (CRN) (see Law and Kelton, 2000), which helps decrease variance and improve the accuracy of determining the labeled action for a state. This is achieved using the same exogenous scenarios for evaluating each action. This approach ensures that the different actions are assessed under the same conditions, thus reducing the variance in the comparison. In addition, DCL integrates a state-of-the-art bandit algorithm, Sequential Halving (SH) (Karnin et al., 2013), to efficiently allocate exogenous scenarios to actions that are more promising to be optimal. This combination of techniques enables DCL to address high stochasticity more effectively.

Additionally, DCL relies on neural networks solely for policy representation, avoiding their use as cost approximators, which can be prone to high noise levels in cost estimates. This design choice enables DCL to avoid issues related to inaccurate cost approximations, concentrating on robust policy representation instead.

We evaluate DCL on three well-known inventory problems: lost sales inventory control, perishable inventory systems, and inventory systems with random lead times. Our results demonstrate that DCL consistently outperforms existing state-of-the-art heuristics and achieves an optimality gap of at most 0.1% for each of these problems, a significant improvement over the 3-6% gap observed with A3C in the lost sales problem (Gijsbrechts et al., 2022). Remarkably, the same set of hyperparameters is used across all experiments, demonstrating the robustness and generalizability of our proposed approach. Furthermore, we find that the combination of Sequential Halving and Common Random Numbers together reduces simulation effort by about two orders of magnitude. This work, therefore, represents a significant advancement in developing a DRL algorithm for inventory management problems, providing efficient solutions for a wide range of challenging scenarios. A key insight arising from this paper is that a single general-purpose algorithm may outperform the best heuristic policies for three difficult inventory problems, which is of interest to practitioners as well as researchers.

This paper is organized as follows: §2 reviews the literature, §3 provides the details of Markov Decision Processes with Exogenous Inputs, and §4 introduces the DCL algorithm. Experimental setup and numerical results are presented in §5 and §6, while §7 concludes the paper.

2 Literature Review

We first discuss well-known heuristic inventory policies for three difficult inventory problems considered in this paper. We then delve into the emerging use of DRL in inventory management.

2.1 Heuristic Policies for three Difficult Inventory Problems

Many leading heuristics for the inventory problems considered in this paper are modifications of the *base-stock policy*, which is prevalent in a wide range of inventory systems due to its inherent simplicity (Clark and Scarf, 1960). It issues an order each period to increase the *inventory position*, which equals inventory on-hand plus inventory in pipeline minus back-orders, to a fixed number known as the *base-stock level*. Its simplicity stems from having only this single parameter, which can either be efficiently optimized or approximated, depending on the model.

Lost sales inventory control is a canonical inventory problem, and its complex stochastic nature has prompted extensive research (see Bijvank and Vis, 2011). Finding the optimal policy for lost sales systems with lead times is impractical because it depends on each outstanding order (Morton, 1969; Zipkin, 2008). Prior studies have established the asymptotic optimality of simple

policies, such as base-stock and constant order policies, as either the penalty cost or the lead-time grows large (Huh et al., 2009; Goldberg et al., 2016; Xin and Goldberg, 2016), but finding optimal policies beyond these regimes remains intractable even for moderately long lead times. Therefore, researchers and practitioners often resort to heuristic approaches. Zipkin (2008) offers a collection of benchmark problems for heuristic evaluation, highlighting the well-performing *myopic* policies (Morton, 1971) in these benchmarks. Xin (2021) studies the *capped base-stock* policy, first introduced by Johansen and Thorstenson (2008), building upon the asymptotic properties of prior approaches. It works akin to the base-stock policy by ordering up to the base-stock level, but it also introduces a cap on the maximum number of orders.

Perishable inventory systems with a fixed product lifetime have triggered much inventory research throughout the years, as shown in comprehensive reviews (Nahmias, 1975a; Karaesmen et al., 2011; Nahmias, 2011; Chao et al., 2018). In these systems, any remaining inventory that reaches the end of its lifetime perishes and is removed with accompanying waste costs. The optimal policy for these systems is particularly intricate, as it necessitates tracking the inventory of each age group due to the fixed product lifetime, resulting in a multidimensional state space (Nahmias, 1975b). Additionally, one needs to consider the *issuance policy*—the order in which items are sold. While the first-in-first-out (FIFO) policy prioritizes selling the oldest items first, the last-in-first-out (LIFO) policy does the opposite by selling the youngest items first. Interestingly, studies focusing on systems under the LIFO policy are sparse (e.g., Cohen and Pekelman, 1978; Bu et al., 2023) despite their common occurrence in retail operations (Minner and Transchel, 2010). Also, standard base-stock policies fall short by considering only the inventory position, failing to account for the age of units in stock and transit.

To fill this gap, Haijema and Minner (2019) introduce *BSP-low-EW*—a modified base-stock policy that leverages the concept of estimated waste, or the expected number of units in inventory that will perish during lead time (Broekmeulen and van Donselaar, 2009). The policy utilizes two order-up-to levels based on the inventory position and factors in the estimated waste during lead time, under the assumption that demand per period is deterministic and equals the mean. As evidenced by a large-scale simulation study across various settings, including different issuing policies, BSP-low-EW emerges as the top-performing heuristic.

Inventory systems with random lead times pose significant challenges, particularly when orders may *cross*, which happens when an order that is placed after another order is received before that order. In the presence of order-crossing, states must include the entire order history (Muthuraman et al., 2015), and consequently, the traditional base-stock policy is no longer optimal (Disney et al., 2016). Yet, heuristic solutions tailored to address these conditions remain scarce (Stolyar and Wang, 2022), and typically the system is optimized within the framework of base-

stock or (r, Q) policies (Bradley and Robinson, 2005; Ang et al., 2017). Stolyar and Wang (2022) propose the *generalized base-stock* (GBS) policy, which sets a dynamic target for the inventory in the pipeline that is adjusted based on the inventory level. This enables the policy to differentiate between the inventory level and the pipeline inventory - a crucial distinction when lead times are stochastic. The GBS policy demonstrates significant cost savings compared to the base-stock policy.

2.2 Deep Reinforcement Learning for Inventory Management

The deep reinforcement learning literature has seen several groundbreaking algorithms, such as Deep Q-Network (DQN) (Mnih et al., 2015), Asynchronous Advantage Actor-Critic (A3C) (Mnih et al., 2016), Proximal Policy Optimization (PPO) (Schulman et al., 2017) and AlphaZero (Silver et al., 2018), demonstrating remarkable performance in diverse domains, including early applications to inventory problems (see Boute et al., 2022).

The potential of deep reinforcement learning is first identified by early work including Oroojlooyjadid et al. (2021), who apply DQN to the beer game, and Gijsbrechts et al. (2022), who apply A3C to three classic inventory problems: lost sales, dual sourcing, and multi-echelon inventory control. With extensive hyperparameter tuning, A3C demonstrates competitive performance against state-of-the-art heuristics, indicating DRL’s promise as a general-purpose technology in this domain. While being outperformed by the capped-base stock and myopic-2 (an extension of the myopic policy) policies for the lost sales problem, the authors find that A3C performs better than the base-stock policy and obtains a 3-6% optimality gap for instances with a computationally feasible optimal policy. In our study, we push the boundary of the state-of-the-art by demonstrating that the proposed DCL algorithm not only achieves substantially lower optimality gaps than the A3C algorithm for the lost sales problem but also surpasses all tested heuristics in a comprehensive simulation study without relying on hyperparameter optimization. Moreover, De Moor et al. (2022) incorporate potential-based reward shaping in the DQN algorithm for perishable inventory systems, showing that shaping from a teacher policy can improve the learning process of a DRL algorithm when a good heuristic like BSP-low-EW is present. However, their shaped-DQN algorithm cannot match the performance of BSP-low-EW in some settings, particularly when the lifetime of a product is large. Conversely, DCL outperforms the BSP-Low-EW policy in each problem instance without requiring sophisticated teacher policies to be present.

Beyond these DRL applications to inventory management, other studies specifically deploy Proximal Policy Optimization (PPO) to address inventory challenges, exhibiting varying degrees of performance efficacy (e.g., Vanvuchelen et al., 2020; van Hezewijk et al., 2023; Geervers et al., 2023). Our research distinguishes itself from these listed applications of deep reinforcement learning (DRL) to inventory management, not merely by applying pre-existing DRL algorithms but by architecting a new algorithm specifically tailored to the unique demands of such problems. In

this vein, AlphaZero provides a relevant comparative framework. Silver et al. (2018) introduced AlphaZero as a general solution for deterministic two-player board games, capitalizing on the known dynamics and rules governing these games. Analogously, our approach, DCL, proposes a general framework for environments impacted by stochastic exogenous inputs featuring a singular decision-maker. This method reflects a concerted effort to enhance the fit between the algorithm design and the inherent characteristics of the inventory management context.

From the methodological perspective, Deep Controlled Learning aligns with a category of algorithms known as classification-based policy iteration (CBPI) (e.g., Lagoudakis and Parr, 2003; Lazaric et al., 2016). These algorithms implement iterative simulations to create datasets comprising states and their estimated optimal actions, enhancing policies through iterative classification tasks. By leveraging simulations, they are equipped to navigate the aforementioned challenges associated with inventory management within the context of DRL. Specifically, the CBPI framework circumvents the need for cost approximation via neural networks instead directly estimating optimal actions.

In addition to harnessing the computational strength of deep neural networks for classification tasks to augment policy representation, DCL substantially extends this framework in two ways. Firstly, DCL innovates by introducing an efficient simulation mechanism. In contrast to the conventional approach that uniformly distributes simulation resources to estimate the optimal action for a given state, utilized by previous CBPI applications, DCL employs a bandit algorithm armed with a variance control mechanism, namely Sequential Halving with Common Random Numbers. By this, DCL optimizes resource allocation during simulations, enabling up to two orders of magnitude reduction in simulation effort. To our knowledge, DCL is the first work that combines and integrates Sequential Halving with Common Random Numbers for optimal action estimation within the deep reinforcement learning context. Secondly, DCL is specifically proposed for MDPs where exogenous inputs significantly influence the environment. We showcase the efficacy and adaptability of DCL by obtaining near-optimal policies in three complex inventory problems while outperforming the best heuristics.

3 Markov Decision Processes with Exogeneous Inputs

We explore a specialized class of Markov Decision Processes that will be referred to as *MDPs with Exogenous Inputs* (MDP-EI). This framework is particularly useful in various operational settings, including inventory management problems, where independent stochastic sources such as demand and lead time significantly influence the decision-making process. We can model these stochastic sources as exogenous inputs to the MDP, providing a robust and flexible framework to analyze and optimize decision-making over time (cf. the unified framework in Powell, 2019). Consequently, our proposed DCL algorithm adopts MDP-EI to model inventory management problems.

In the MDP-EI setting, we consider a finite discrete state space \mathcal{S} , a finite action space $\mathcal{A} = \{0, 1, \dots, m\}$, and a set of possible exogenous inputs \mathcal{W} . For any given state $\mathbf{s} \in \mathcal{S}$, we represent the applicable actions as $\mathcal{A}_{\mathbf{s}} \subseteq \mathcal{A}$. A deterministic policy, denoted by π , is a function $\pi : \mathcal{S} \rightarrow \mathcal{A}$ that assigns to each state \mathbf{s} a valid action $\pi(\mathbf{s}) \in \mathcal{A}_{\mathbf{s}}$. In each period t , the next state \mathbf{s}_{t+1} and the incurred cost c_t are determined by a combination of the current state \mathbf{s}_t , the action a_t taken, and the exogenous input ξ_t . Here, $\xi_t \in \mathcal{W}$ represents an exogenous stochastic input of any dimension observed after the execution of action a_t at period t . These inputs are assumed to be independent of the states and actions. For ease of exposition, we shall also assume that the inputs are independently and identically distributed, which is a common assumption in inventory management literature (see Zipkin, 2000) and in practical settings (e.g., Van Houtum and Kranenburg, 2015). Consequently, following the policy π from state \mathbf{s} results in a random trajectory composed of states, actions, exogenous inputs, and costs. This trajectory, representing the evolution of the system, can be described by the sequence $(\mathbf{s}_0, a_0, \xi_0, c_0, \mathbf{s}_1, a_1, \xi_1, c_1, \mathbf{s}_2, a_2, \xi_2, c_2, \mathbf{s}_3, \dots)$, where $\mathbf{s}_0 = \mathbf{s}$ and $a_t = \pi(\mathbf{s}_t)$. See Figure 1 for the visual depiction of this evolution.

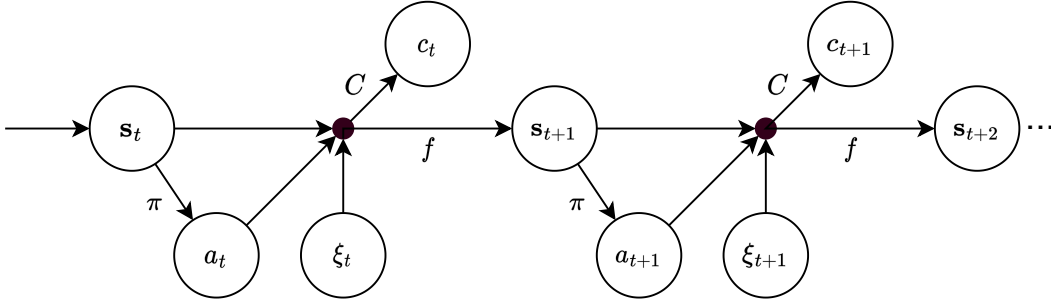


Figure 1: Graphical representation of the MDP-EI, with arrows indicating direct dependence.

Accordingly, we define the MDP-EI as a tuple $\mathcal{M} = \langle \mathcal{S}, \mathcal{A}, \mathcal{W}, \Xi, f, C, \alpha, \mathbf{s}_0 \rangle$. Here, \mathcal{S} and \mathcal{A} denote the finite sets of states and actions, respectively, while \mathcal{W} is the set of exogenous inputs. The variable Ξ represents a generic random variable such that $\xi_t \sim \Xi$. We shall assume that Ξ is distributed such that realizations $\xi_t \sim \Xi$ can be generated efficiently. State transitions are determined by the function $f : \mathcal{S} \times \mathcal{A} \times \mathcal{W} \rightarrow \mathcal{S}$. This function maps a state-action-input tuple (\mathbf{s}, a, ξ) to a new state $\mathbf{s}' = f(\mathbf{s}, a, \xi)$. The cost function $C : \mathcal{S} \times \mathcal{A} \times \mathcal{W} \rightarrow \mathbb{R}$ assigns a cost $c = C(\mathbf{s}, a, \xi)$ to each state-action-input combination. Based on this formalization, we can derive the state transition probability and the expected cost when executing action a in state \mathbf{s} as follows:

$$\mathbf{P}(\mathbf{s}' | \mathbf{s}, a) = \mathbf{E}_{\xi \sim \Xi}[\mathbb{1}_{[\mathbf{s}' = f(\mathbf{s}, a, \xi)]}], \quad \mathbf{s}, \mathbf{s}' \in \mathcal{S}, a \in \mathcal{A}_{\mathbf{s}}, \quad (1)$$

$$\bar{C}(\mathbf{s}, a) = \mathbf{E}_{\xi \sim \Xi}[C(\mathbf{s}, a, \xi)], \quad \mathbf{s} \in \mathcal{S}, a \in \mathcal{A}_{\mathbf{s}}. \quad (2)$$

In the MDP-EI formalization, costs accumulate over an infinite horizon. Let $\alpha \in (0, 1]$ denote the

discount factor. For $\alpha < 1$, costs are discounted, while $\alpha = 1$ corresponds to the average cost criterion. We assume that the system starts from an initial state \mathbf{s}_0 , which could be deterministic or random with an arbitrary distribution, depending on the specific problem context. An example next illustrates these concepts.

Example: We consider the well-known discrete-time lost sales inventory system (Zipkin, 2008), which can be characterized as an MDP-EI model $\mathcal{M} = \langle \mathcal{S}, \mathcal{A}, \mathcal{W}, \Xi, f, C, \alpha, \mathbf{s}_0 \rangle$. In this system, we manage an inventory of items over time by placing orders for new items, attempting to meet the exogenous demands, and incurring costs based on whether we have sufficient inventory to meet the demand or not. The lead time for new orders to arrive is greater than one period (i.e., $\tau > 1$). In this setting, states \mathbf{s} are represented as vectors in \mathbb{R}^τ , where each element of the vector represents a component of the inventory: $\mathbf{s}[1]$ corresponds to on-hand inventory or the current availability of items, and $\mathbf{s}[2]$ to $\mathbf{s}[\tau]$ depict pipeline inventory, which are the items ordered and due to arrive in $1, \dots, \tau - 1$ future periods, respectively. For this system, the per-period demand, denoted by D , acts as the generic random variable Ξ , and we have $\xi \sim D$ with the exogenous input space $\mathcal{W} := \mathbb{Z}_0$. The transition function $f(\mathbf{s}, a, \xi) = \mathbf{s}'$ describes the evolution of the state when an action a is taken in state \mathbf{s} under demand ξ . The on-hand inventory is updated by meeting the demand with the current on-hand inventory and then adding any pipeline inventory due to arrive, leading to $\mathbf{s}'[1] = (\mathbf{s}[1] - \xi)^+ + \mathbf{s}[2]$. Action a corresponds to the order due to arrive in τ time periods, hence $\mathbf{s}'[\tau] = a$. For all $i \in \{2, \dots, \tau - 1\}$, pipeline inventory is shifted one period closer to arrival, with $\mathbf{s}'[i] = \mathbf{s}[i + 1]$. The transition function is therefore given as $f((\mathbf{s}[1], \dots, \mathbf{s}[\tau]), a, \xi) := ((\mathbf{s}[1] - \xi)^+ + \mathbf{s}[2], \mathbf{s}[3], \dots, \mathbf{s}[\tau], a)$. The cost function is $C(\mathbf{s}, a, \xi) = h(\mathbf{s}[1] - \xi)^+ + p(\xi - \mathbf{s}[1])^+$, where h is the unit cost of holding inventory and p is the unit penalty cost of lost sales. (In this case, action a does not directly influence the cost in the current period.)

4 Algorithm

In §4.1, we discuss policy iteration and approximate policy iteration. In §4.2, we motivate and discuss Deep Controlled Learning and explain the key ideas underlying its development.

4.1 Approximate Policy Iteration

Policy iteration, a fundamental concept in Markov Decision Processes, is an iterative method that continually evaluates and improves a given policy to find the optimal solution and will be discussed next in the context of our MDP-EI setting with $\alpha < 1$. In this setting, following a policy π from an initial state \mathbf{s} results in a random trajectory. The discounted costs accumulated over such a trajectory, with initial state $\mathbf{s}_0 = \mathbf{s}$, can be expressed as follows:

$$V_\pi(\mathbf{s}) := \sum_{t=0}^{\infty} \alpha^t c_t, \text{ with } a_t = \pi(\mathbf{s}_t), \xi_t \sim \Xi, c_t = C(\mathbf{s}_t, a_t, \xi_t), \text{ and } \mathbf{s}_{t+1} = f(\mathbf{s}_t, a_t, \xi_t). \quad (3)$$

We introduce two essential concepts: the *value function* and the *action-value function*. The value function $v_\pi(\mathbf{s})$ for policy π represents the expected value of $V_\pi(\cdot)$ over the exogenous inputs ξ , that is, $v_\pi(\mathbf{s}) = \mathbf{E}_\xi[V_\pi(\mathbf{s})]$. This function conveys the expected discounted costs over an infinite horizon, starting from state \mathbf{s} and following policy π , which satisfies (see Puterman, 2014, for details):

$$v_\pi(\mathbf{s}) = \bar{C}(\mathbf{s}, \pi(\mathbf{s})) + \alpha \sum_{\mathbf{s}' \in \mathcal{S}} \mathbf{P}(\mathbf{s}'|\mathbf{s}, \pi(\mathbf{s})) v_\pi(\mathbf{s}'), \quad \forall \mathbf{s} \in \mathcal{S}. \quad (4)$$

While the value function provides an overall measure of policy performance, assessing the value of individual actions can be useful, leading us to the action-value function concept. The action-value function $q_\pi(\mathbf{s}, a)$ represents the expected value of $Q_\pi(\mathbf{s}, a)$, where $Q_\pi(\mathbf{s}, a)$ denotes the costs incurred over a trajectory with initial state $\mathbf{s}_0 = \mathbf{s}$ and initial action $a_0 = a$:

$$Q_\pi(\mathbf{s}, a) := \sum_{t=0}^{\infty} \alpha^t c_t, \quad \text{with } a_{t,t>0} = \pi(\mathbf{s}_t), \quad \xi_t \sim \Xi, \quad c_t = C(\mathbf{s}_t, a_t, \xi_t), \quad \text{and } \mathbf{s}_{t+1} = f(\mathbf{s}_t, a_t, \xi_t). \quad (5)$$

Hence, the action-value function $q_\pi(\mathbf{s}, a)$ can be expressed as (see Puterman, 2014, for details):

$$q_\pi(\mathbf{s}, a) = \bar{C}(\mathbf{s}, a) + \alpha \sum_{\mathbf{s}' \in \mathcal{S}} \mathbf{P}(\mathbf{s}'|\mathbf{s}, a) v_\pi(\mathbf{s}'), \quad \forall \mathbf{s} \in \mathcal{S}, \quad \forall a \in \mathcal{A}_\mathbf{s}. \quad (6)$$

These equations essentially establish a relationship between the action-value and value functions, and the transition probabilities (1) and expected costs (2) of a particular state-action pair (\mathbf{s}, a) , as stated in the MDP-EI framework in §3.

An improved policy, denoted as $\pi^+(\cdot)$, is one that minimizes $q_\pi(\mathbf{s}, a)$ for all possible states \mathbf{s} :

$$\pi^+(\mathbf{s}) := \arg \min_{a \in \mathcal{A}_\mathbf{s}} q_\pi(\mathbf{s}, a), \quad \forall \mathbf{s} \in \mathcal{S} \quad (7)$$

Note that $\pi^+(\mathbf{s})$ indicates the optimal action to take in state \mathbf{s} before adopting policy π for subsequent states. In cases of ties in the argmin operation, we can break them arbitrarily, for instance, by opting for the smallest action. Repeated improvement of a policy in this manner is known as *policy iteration* and leads to the optimal policy under a broad range of assumptions (Puterman, 2014). Nonetheless, this approach requires the calculation of the action-value function $q_\pi(\mathbf{s}, a)$ for each state-action pair (\mathbf{s}, a) , $\mathbf{s} \in \mathcal{S}$, $a \in \mathcal{A}$, which involves resolving the system of equations (4). The latter task can become computationally challenging when the state space \mathcal{S} is large, creating a demand for more efficient strategies.

Approximate policy iteration strategies address the computational burden inherent in exact policy iteration by estimating the action-value function and approximating the improved policy.

The goal is to avoid solving the system of equations (4) and to refrain from estimating the action-value function for every possible state-action pair, respectively. These adjustments make approximate policy iteration accessible for large state spaces.

We first focus on estimating the action-value function for a given state-action pair (\mathbf{s}, a) . A prominent approach for this task is the application of *rollout simulations*, a method first proposed by Tesauro and Galperin (1996). Within the context of MDPs with Exogenous Inputs, rollout simulations facilitate the generation of numerous independent replications of the trajectory cost (5), each under a unique exogenous scenario. The empirical mean of these replications offers an estimate of the action-value function, a process we have previously referred to as *evaluating states under multiple exogenous scenarios* in §1. This process thus provides a practical way of incorporating the effects of varying exogenous scenarios into our action-value function estimates.

In order to facilitate these simulations and obtain realizations of the trajectory costs, we require an approximation approach, given that MDP-EI are modeled with an infinite horizon (see §3). To facilitate this, we truncate the trajectory length after H steps, thereby setting a finite horizon. Given the distribution of exogenous inputs Ξ , we can generate an exogenous scenario ξ of length H as follows:

$$\xi = \{\xi_0, \xi_1, \dots, \xi_{H-1}\}, \text{ with } \forall t \in \{0, \dots, H-1\} : \xi_t \sim \Xi. \quad (8)$$

We can then approximate $Q_\pi(\mathbf{s}, a)$ by initiating the trajectory in state $\mathbf{s}_0 = \mathbf{s}$, taking action $a_0 = a$, and summing the discounted costs over the finite horizon and under the exogenous scenario ξ :

$$\hat{Q}_\pi(\mathbf{s}, a | \xi) := \sum_{t=0}^{H-1} \alpha^t c_t, \text{ with } a_{t,t>0} = \pi(\mathbf{s}_t), \ c_t = C(\mathbf{s}_t, a_t, \xi_t), \text{ and } \mathbf{s}_{t+1} = f(\mathbf{s}_t, a_t, \xi_t). \quad (9)$$

The approximated trajectory costs for a state-action pair often exhibit considerable variance due to the diverse exogenous scenarios. To mitigate this variability and improve the precision of the action-value function estimation, it is advantageous to generate numerous exogenous scenarios, each yielding a distinct approximate trajectory cost. Inadequate estimation of the action-value functions could hinder policy improvement, which requires identifying the action that minimizes action-value function $q_\pi(\mathbf{s}, a)$ for a given state \mathbf{s} . This is especially applicable to the previously mentioned DRL approaches, such as DQN, A3C, and PPO, as these approaches rely on a single scenario for both the estimation of action-value functions and policy updates. The potential pitfalls of this practice and the benefit of averaging multiple scenarios become evident in the context of the previously introduced lost sales inventory model:

Example (continued): Recall the aforementioned lost sales inventory model, formulated as an MDP with Exogenous Inputs in §3. Consider a system with lead time $\tau = 2$, where the applicable

actions are $a \in \mathcal{A} = \{0, 1\}$, and in each period, and we observe demand $\xi \in \mathcal{W} = \{0, 1\}$. We define the per unit holding cost $h = 1$, and per unit penalty cost $p = 9$. We adopt the average-cost criterion, i.e., $\alpha = 1.0$. Initially, we have one unit of on-hand inventory and no unit in the pipeline, $\mathbf{s}_0 = (1, 0)$. In this setting, we start with an initial policy π , which consistently places an order of 1 unit irrespective of the current state. Our objective is to examine how this policy can be improved for state \mathbf{s}_0 by estimating the action-value function of both actions, $a = 0$ and $a = 1$. Table 1 shows the approximate trajectory costs of $a = 0, 1$ under three generated exogenous scenarios. We set the horizon length $H = 4$, and approximate the trajectory costs as $\hat{Q}_\pi(\mathbf{s}, a|\boldsymbol{\xi}) = \sum_{t=0}^3 c_t$. While for scenarios $\boldsymbol{\xi}_1$ and $\boldsymbol{\xi}_2$, action $a = 0$ yields lower approximate trajectory costs than action $a = 1$, in scenario $\boldsymbol{\xi}_3$, action $a = 1$ actually results in a much lower approximate trajectory cost than action $a = 0$. Consequently, when taking averages of the trajectory cost over three exogenous scenarios to obtain action-value estimates for actions, we observe that action $a = 1$ has a lower action-value estimate, such that $\hat{q}_\pi(\mathbf{s}, a|\mathbf{s} = \mathbf{s}_0, a = 1) = 6.33$ where $\hat{q}_\pi(\mathbf{s}, a|\mathbf{s} = \mathbf{s}_0, a = 0) = 8$. As demonstrated in this case, considering multiple exogenous scenarios during the policy improvement process can prevent the selection of an inferior action that may appear superior under limited scenarios.

		Scenarios														
		$\boldsymbol{\xi}_1 = \{0, 0, 0, 0\}$					$\boldsymbol{\xi}_2 = \{0, 1, 0, 1\}$					$\boldsymbol{\xi}_3 = \{1, 1, 1, 1\}$				
		\mathbf{s}_t	a_t	ξ_t	c_t	\hat{Q}_π	\mathbf{s}_t	a_t	ξ_t	c_t	\hat{Q}_π	\mathbf{s}_t	a_t	ξ_t	c_t	\hat{Q}_π
Action $a = 0$	$t = 0$	(1, 0)	0	0	1		(1, 0)	0	0	1		(1, 0)	0	1	0	
	$t = 1$	(1, 0)	1	0	1		(1, 0)	1	1	0		(0, 0)	1	1	9	
	$t = 2$	(1, 1)	1	0	1		(0, 1)	1	0	0		(0, 1)	1	1	9	
	$t = 3$	(2, 1)	1	0	2	5	(1, 1)	1	1	0	1	(1, 1)	1	1	0	18
Action $a = 1$	$t = 0$	(1, 0)	1	0	1		(1, 0)	1	0	1		(1, 0)	1	1	0	
	$t = 1$	(1, 1)	1	0	1		(1, 1)	1	1	0		(0, 1)	1	1	9	
	$t = 2$	(2, 1)	1	0	2		(1, 1)	1	0	1		(1, 1)	1	1	0	
	$t = 3$	(3, 1)	1	0	3	7	(2, 1)	1	1	1	3	(1, 1)	1	1	0	9

Table 1: The approximated trajectory costs of actions under various exogenous scenarios. ($\hat{Q}_\pi(\mathbf{s}_0, a|\boldsymbol{\xi})$ is displayed as \hat{Q}_π .)

We next outline an approximate policy iteration algorithm that shall be refined in §4.2. Suppose we generate M independent rollout simulations to estimate the action-value function. Each rollout involves generating an exogenous scenario $\boldsymbol{\xi}_r$, $r = 1, \dots, M$ (8), and computing the trajectory cost $\hat{Q}_\pi(\mathbf{s}, a|\boldsymbol{\xi}_r)$ (9). The resulting estimate of the action-value function for state \mathbf{s} satisfies:

$$\hat{q}_\pi(\mathbf{s}, a) = \sum_{r=1}^M \frac{1}{M} \hat{Q}_\pi(\mathbf{s}, a|\boldsymbol{\xi}_r), \quad \forall a \in \mathcal{A}_\mathbf{s}. \quad (10)$$

Subsequently, the improved action for state \mathbf{s} before following policy π can then be estimated as $\hat{\pi}^+(\mathbf{s}) := \arg \min_{a \in \mathcal{A}_\mathbf{s}} \hat{q}_\pi(\mathbf{s}, a)$, where $\hat{\pi}^+(\mathbf{s})$ is referred to as the *simulation-based action* for

state \mathbf{s} (cf. (7)). However, obtaining the simulation-based action for each state in \mathcal{S} may be computationally prohibitive. To circumvent this, we sample N states from the state space \mathcal{S} and compute the corresponding simulation-based action for each sampled state.

Still, the simulation-based policy, denoted as $\hat{\pi}^+(\cdot)$, covers only the sampled states. To extend this to the entire state space, \mathcal{S} , a function approximation is required that can offer a policy representation applicable to all states (Boute et al., 2022). The policy approximation issue is addressed as a classification task, whereby a classification model with parameters θ is trained to map states to actions, thereby approximating the policy $\hat{\pi}^+(\cdot)$. The model training utilizes the collected samples as a set of *data points* $\mathcal{K} = \{(\mathbf{s}_k, \hat{\pi}^+(\mathbf{s}_k)) | k \in 1, \dots, N\}$, instructing the classifier to map states to actions congruent with the simulation-based policy $\hat{\pi}^+(\cdot)$. The resultant policy, π_θ , serves as a viable approximation of the policy $\hat{\pi}^+(\cdot)$ for all states in \mathcal{S} .

The policy improvement process and function approximation provide a refined strategy for navigating complex, multi-dimensional state spaces. However, their practical application requires careful consideration of computational complexity and approximation accuracy, which hinge on parameters H , M , and N . We next delve deeper into DCL and explain its strategies to overcome practical challenges.

4.2 Deep Controlled Learning

While Lazaric et al. (2016) demonstrate that increasing any of H (the horizon length), M (the number of exogenous scenarios per state-action pair), and N (the number of states to be sampled) theoretically enhances the policy improvement process, DCL focuses on optimizing the framework’s practical performance with fixed H , M , and N specifically for solving MDP-EI. In this way, DCL seeks to deliver higher performance levels without overburdening computational resources, thereby boosting the algorithm’s efficiency.

Algorithm 1 provides a detailed description of the Deep Controlled Learning framework. Given an MDP-EI model \mathcal{M} , an initial policy π_0 , and a selection of hyperparameters, including H , M , and N , DCL executes n steps of approximate policy improvement, indexed by $i = 0, 1, \dots, n - 1$. This process iteratively refines the initial policy. During each iteration i , DCL begins by gathering N data samples $\mathcal{K}_i = \{(\mathbf{s}_k, \hat{\pi}_i^+(\mathbf{s}_k)) | k \in \{1, \dots, N\}\}$. This collection of samples constitutes states and their corresponding simulation-based actions. Subsequently, DCL generates the policy π_{i+1} by training a neural network *classifier*, i.e., a neural network that can prescribe an action for any state. This classifier works to approximate the simulation-based policy reflected by the dataset.

In the remainder of this section, we first demonstrate how DCL leverages modern hardware capabilities to sample states as efficiently as possible and clarify the selection process of states \mathbf{s} for inclusion in the data set \mathcal{K} . Next, we explain using the Sequential Halving algorithm with Common Random Numbers to determine the simulation-based action for each sampled state. Finally, we

describe the application of neural networks as classification algorithms for policy representation.

Algorithm 1 Deep Controlled Learning

```

1: Input: MDP model:  $\mathcal{M} = \langle \mathcal{S}, \mathcal{A}, \mathcal{W}, \Xi, f, C, \alpha, \mathbf{s}_0 \rangle$ , initial policy:  $\pi_0$ , neural network structure:  $N_\theta$ , number of approximate policy iterations:  $n$ , number of states to be collected:  $N$ , number of exogenous scenarios per state-action pairs:  $M$ , depth of the rollouts (horizon length):  $H$ , length of the warmup period:  $L$ , number of workers:  $w$ 
2: for  $i = 0, 1, \dots, n - 1$  do
3:    $\mathcal{K}_i = \{\}$ , the dataset
4:   for each  $worker = 1, \dots, w$  do in parallel ▷ parallelization
5:      $\mathbf{s}_1 = \text{SampleStartState}(\mathcal{M}, \pi_i, L)$  ▷ sample starting state
6:     Generate exogenous scenario  $\xi$  by (8),  $|\xi| = \lceil N/w \rceil$ 
7:     for  $k = 1, \dots, \lceil N/w \rceil$  do
8:       Find  $\hat{\pi}_i^+(\mathbf{s}_k) = \text{Simulator}(\mathcal{M}, \mathbf{s}_k, \pi_i, M, H)$  ▷ SH with CRN
9:       Add  $(\mathbf{s}_k, \hat{\pi}_i^+(\mathbf{s}_k))$  to the data set  $\mathcal{K}_i$ 
10:       $\mathbf{s}_{k+1} = f(\mathbf{s}_k, \hat{\pi}_i^+(\mathbf{s}_k), \xi_{k-1})$ 
11:    end for
12:  end for
13:   $\pi_{i+1} = \text{Classifier}(N_\theta, \mathcal{K}_i)$  ▷ training neural networks
14: end for
15: Output:  $\pi_1, \dots, \pi_n$ 

```

State sampling

DCL deploys a suite of strategies for efficient state sampling and effective dataset construction. Central to this is DCL’s capability to parallelize the process that combines state sampling with identifying corresponding simulation-based actions. In particular, DCL enables simultaneous sampling of a multitude of states and actions by adopting an approach akin to AlphaZero (see Silver et al., 2018), which concurrently runs multiple game simulations using the same neural network across different processor cores. In DCL, this is achieved by distributing the simulation process, involving selecting a state for the dataset and finding its simulation-based action, across several computational threads, allowing for optimal utilization of vast computing clusters and supercomputers. Regarding implementation, DCL assigns the task of sampling state-action pairs uniformly to available worker threads. Specifically, each worker thread is responsible for sampling $\lceil N/w \rceil$ state-action pairs, where N is the total number of samples to be collected, and w denotes the accessible computing threads (as shown on Line 4 in Algorithm 1).

We first describe how each worker thread samples its first state, \mathbf{s}_1 , for inclusion in the dataset. Given an initial state \mathbf{s}_0 specified by the MDP-EI model \mathcal{M} , each worker thread generates an exogenous scenario ξ of length L (a hyperparameter of the algorithm), starting from the initial state \mathbf{s}_0 , and follows the current policy π_i through this trajectory. The state observed at the end of the trajectory is used as the starting state (as depicted in Algorithm 2, invoked on Line 5 in Algorithm 1), which is subsequently incorporated into the dataset after finding its simulation-based

action. With this approach, each thread starts from a distinct state, facilitating comprehensive coverage of the state space. Such inclusivity of a broad range of states results in a robust policy that is relevant to various scenarios and states (Sutton and Barto, 2018).

Algorithm 2 SampleStartState

```

1: Input:  $\mathcal{M}, \pi, L$ 
2: Generate an exogenous scenario  $\xi$  by (8),  $|\xi| = L$ 
3: for  $j = 0, \dots, L - 1$  do
4:    $\mathbf{s}_{j+1} = f(\mathbf{s}_j, \pi(\mathbf{s}_j), \xi_j)$ 
5: end for
6: Output:  $\mathbf{s}_L$ 

```

The creation of the remaining states for \mathcal{K}_i is influenced by the simulation-based policy $\hat{\pi}_i^+(\cdot)$, rather than the current policy π_i . Each worker thread generates and retains an exogenous scenario ξ , transitioning to a new state once the simulation-based action for the sampled state has been identified (as shown on Lines 6 and 10 in Algorithm 1). This strategy ensures that the policy improvement is meaningful and applicable in the context of the states that the system is likely to visit in practice (Ernst et al., 2005). In other words, it helps ensure that the improved policy is not merely theoretically effective but also practically relevant to the actual operation of the system.

Identifying simulation-based actions

Once a state \mathbf{s} for the data set is selected, DCL identifies the corresponding simulation-based action $\hat{\pi}^+(\mathbf{s})$ by locating the action associated with the lowest estimate of the action-value function. In performing this task, DCL maintains a fixed budget of exogenous scenarios, determined by the hyperparameter M , to prevent an escalation in computational resource consumption. Furthermore, approximated trajectory costs in MDP-EI may exhibit considerable variance, even when the budget for exogenous scenarios is high, which could result in suboptimal actions being identified as simulation-based actions. In such a context, enhancing the accuracy of the simulation-based action $\hat{\pi}^+(\mathbf{s})$ —to either match the optimal action $\pi^+(\mathbf{s})$ or perform similarly—becomes challenging. To achieve this, DCL utilizes a variance control mechanism, Common Random Numbers, which serves to mitigate the variance in trajectory costs. Additionally, DCL employs a state-of-the-art bandit algorithm, Sequential Halving, to allocate exogenous scenarios to actions that demonstrate greater potential for optimality, avoiding the waste of exogenous scenarios on the suboptimal actions. Algorithm 3 elucidates the specifics of Sequential Halving and the way Common Random Numbers are integrated within its framework.

Common Random Numbers

Common Random Numbers (CRN) is a variance reduction technique frequently used in simulation studies. This method employs the same sequence of random numbers across distinct scenarios to decrease variance and enhance the reliability of comparative evaluations (Law and Kelton,

Algorithm 3 Simulator

```
1: Input:  $\mathcal{M}, \mathbf{s}, \pi, M, H$ 
2: Initialize: Total rollout budget:  $B_s = M|\mathcal{A}_s|$ , number of rollouts allocated to competing
   actions:  $T = 0$ , sum of the approximate trajectory costs for action  $a$ ,  $a \in \mathcal{A}_s$ :  $\tilde{Q}_\pi(\mathbf{s}, a) = 0$ ,
   initial set of competing actions:  $\mathcal{A}_0 = \mathcal{A}_s$ 
3: for  $r = 0, 1, \dots, \lceil \log_2 |\mathcal{A}_s| \rceil - 1$  do ▷ Sequential Halving
4:    $t_r = \left\lceil \frac{B_s}{|\mathcal{A}_r| \lceil \log_2 |\mathcal{A}_s| \rceil} \right\rceil$ , the number exogenous scenarios assigned to each in action in  $\mathcal{A}_r$ 
5:   for  $t = 1, \dots, t_r$  do
6:     Generate an exogenous scenario  $\xi$  by (8),  $|\xi| = H$  ▷ Common Random Numbers
7:     for all  $a \in \mathcal{A}_r$  do
8:       Find  $\hat{Q}_\pi(\mathbf{s}, a|\xi)$  by (9)
9:        $\tilde{Q}_\pi(\mathbf{s}, a) = \tilde{Q}_\pi(\mathbf{s}, a) + \hat{Q}_\pi(\mathbf{s}, a|\xi)$ 
10:    end for
11:  end for
12:   $T = T + t_r$ 
13:   $\hat{q}_\pi(\mathbf{s}, a) = \tilde{Q}_\pi(\mathbf{s}, a)/T, \forall a \in \mathcal{A}_r$ 
14:   $\mathcal{A}_{r+1} = \arg \min_{a \in \mathcal{A}_r}^{1.. \lceil \mathcal{A}_r/2 \rceil} \hat{q}_\pi(\mathbf{s}, a)$  ▷ eliminate half of the actions
15: end for
16: Output: action in  $\mathcal{A}_{\lceil \log_2 |\mathcal{A}_s| \rceil}$ 
```

2000). In the context of the lost sales inventory control application discussed in §3 and §4.1, this entails comparing the approximated trajectory costs of different actions using the *same* demand sequence rather than generating them independently. Understanding the efficacy of this approach requires considering that estimating $\arg \min_{a \in \mathcal{A}_s} \hat{q}_\pi(\mathbf{s}, a)$ involves evaluating whether $\hat{q}_\pi(\mathbf{s}, a) - \hat{q}_\pi(\mathbf{s}, a')$ is greater or less than zero for all pairs of actions $a, a' \in \mathcal{A}_s$. To illustrate this, let us consider two actions $a, a' \in \mathcal{A}_s$. Let ξ_r for $r = 1, \dots, M$ represent independent exogenous scenarios, and let X denote the resulting estimator of $\hat{q}_\pi(\mathbf{s}, a) - \hat{q}_\pi(\mathbf{s}, a')$. In other words, $X = \frac{1}{M} \sum_{r=1}^M (\hat{Q}_\pi(\mathbf{s}, a|\xi_r) - \hat{Q}_\pi(\mathbf{s}, a'|\xi_r))$. Hence, we have $\mathbf{E}[X] = \hat{q}_\pi(\mathbf{s}, a) - \hat{q}_\pi(\mathbf{s}, a')$ and

$$\text{var}[X] = \text{var}[\hat{Q}_\pi(\mathbf{s}, a|\xi)] + \text{var}[\hat{Q}_\pi(\mathbf{s}, a'|\xi)] - 2 \text{cov}[\hat{Q}_\pi(\mathbf{s}, a|\xi), \hat{Q}_\pi(\mathbf{s}, a'|\xi)]. \quad (11)$$

The covariance term, emerging due to the pairwise comparison of the approximate trajectory costs, can be substantial relative to the variance terms, particularly for MDPs with Exogenous Inputs. As such, variance control has the potential to calibrate the variance of the estimator X to an appropriate level for discerning whether action a is superior to action a' .

A straightforward intuition suggests that the covariance term may be positive in many inventory management problems. In such scenarios, actions typically denote the quantity ordered in a period. When comparing actions across diverse exogenous demand sequences, a positive covariance between actions a and a' suggests that their associated approximate trajectory costs will exhibit similar patterns under analogous demand sequences. For instance, under a sequence characterized by

high demand, the corresponding trajectory costs for each action would be elevated compared to those under a sequence with low demand. This intuition for the potential benefits of CRN will be confirmed in numerical results in §6.2, and is illustrated by the following example.

Example (continued): For the numerical example of §4.1, Common Random Numbers enable the generation of the same exogenous scenarios for both applicable actions $a = 0$ and $a = 1$. Given the state \mathbf{s}_0 , the approximate trajectory costs for action $a = 0$ are calculated as 5, 3, and 18, giving $\text{var}[\hat{Q}_\pi(\mathbf{s}_0, 0|\boldsymbol{\xi})] = 52.66$. The approximate trajectory costs for action $a = 1$ are 7, 5, and 9, yielding $\text{var}[\hat{Q}_\pi(\mathbf{s}_0, 1|\boldsymbol{\xi})] = 6.22$. The realizations for the estimator $X = \hat{q}_\pi(\mathbf{s}_0, 1) - \hat{q}_\pi(\mathbf{s}_0, 0)$, can be found as 2, 2 and -9, resulting in $\text{var}[X] = 26.87$. Since $\text{var}[X] < \text{var}[\hat{Q}_\pi(\mathbf{s}_0, 0|\boldsymbol{\xi})] + \text{var}[\hat{Q}_\pi(\mathbf{s}_0, 1|\boldsymbol{\xi})]$ ($26.87 < 52.66 + 6.22$), employing CRN is beneficial for this problem instance.

Sequential Halving

To determine the simulation-based action for a sampled state \mathbf{s} , DCL operates under a fixed budget of exogenous scenarios, $B_{\mathbf{s}} = M|\mathcal{A}_{\mathbf{s}}|$. We denote $B_{\mathbf{s}}$ as the total rollout budget for state \mathbf{s} . A naive approach would distribute the same number of independent exogenous scenarios (M) to each action (e.g., Lagoudakis and Parr, 2003; Lazaric et al., 2016), which can be called as *uniform allocation* strategy. However, as we accumulate statistical data, it might become apparent that certain actions are suboptimal. Allocating limited resources under a specific budget to identify the optimal action from a set, as encountered in this study, has been extensively explored in the literature under the umbrella terms *best arm identification in multi-armed bandits* (cf. Bubeck and Cesa-Bianchi, 2012), and *ranking and selection under fixed budget* (cf. Hong et al., 2021). Since its inception, *Sequential Halving* (Karnin et al., 2013) has emerged as a preferred method in this field, demonstrating its prowess in environments necessitating swift resource allocation (e.g., Danihelka et al., 2022, for its effect in reducing the simulation effort exhibited by AlphaZero).

Accordingly, DCL employs Sequential Halving to circumvent the unnecessary usage of computational resources on suboptimal actions. This algorithm assigns exogenous scenarios to the more promising actions based on their empirical average expected costs, while concurrently accounting for the aforementioned variance control scheme (CRN). Specifically, given a state \mathbf{s} and the feasible action set $\mathcal{A}_{\mathbf{s}}$, the algorithm evenly distributes the total budget $B_{\mathbf{s}}$ across $\log_2 |\mathcal{A}_{\mathbf{s}}|$ rounds and eliminates the lower-performing half of the actions at the end of each round. Within a round, the actions are allocated an identical number of exogenous scenarios. For each scenario, we retain the exogenous inputs (CRN) and calculate the approximate trajectory costs (9) for the competing actions in that round.

DCL diverges from the original Sequential Halving algorithm (see Karnin et al., 2013) in terms of statistics storage. Rather than discarding the collected approximate trajectory costs of the competing actions at the onset of a round, DCL *stockpiles* (Fabiano and Cazenave, 2022) them by

maintaining the sum of the trajectory costs for the actions, such that $\tilde{Q}_\pi(\mathbf{s}, a) = \sum_{i=1}^T \hat{Q}_\pi(\mathbf{s}, a | \xi_i)$, where T represents the number of exogenous scenarios assigned for action $a \in \mathcal{A}_r$ until the end of round r , and \mathcal{A}_r denotes the set of competing actions in round r (cf. Line 9 in Algorithm 3). This helps to decrease the variance term (11) further as we collect more trajectory costs for the actions.

After the last round of Sequential Halving, the single remaining action is identified as the simulation-based action $\hat{\pi}^+(\mathbf{s})$, corresponding to the selected state \mathbf{s} . This state-action pair is subsequently incorporated into the dataset. DCL can efficiently and robustly construct its dataset $\mathcal{K}_i = \{(\mathbf{s}_k, \hat{\pi}_i^+(\mathbf{s}_k)) | k \in \{1, \dots, N\}\}$ at iteration i by systematically following this process, which entails sampling a state and determining its simulation-based action. This dataset is then utilized in the subsequent stage of training neural networks to formulate a policy representation.

Policy approximation with neural networks

Upon construction of the dataset $\mathcal{K}_i = \{(\mathbf{s}_k, \hat{\pi}_i^+(\mathbf{s}_k)) | k \in \{1, \dots, N\}\}$, DCL initiates the training of a neural network to approximate the simulation-based policy $\hat{\pi}^+(\cdot)$. Specifically, given a pre-defined network structure N_θ , the objective is to update the parameters θ such that the resulting policy $\pi_\theta(\cdot)$ closely aligns with the simulation-based policy $\hat{\pi}^+(\cdot)$ within the states present in \mathcal{K}_i . With a sufficiently large number of samples (N) and appropriate training, the neural network may provide generalization across the entire state space \mathcal{S} (Boute et al., 2022). Unlike other versions of approximate policy iteration, our machine learning model solves a classification task, which may contribute to stable training and good generalization. For training neural networks, we adopt a standard set of strategies (see Goodfellow et al., 2016); we refer readers to Appendix A for the details, including the specifics of the *Classifier* algorithm (Line 13 in Algorithm 1).

After completion of training, the neural network policy is defined as $\pi_\theta(\mathbf{s}) = \arg \max_{a \in \mathcal{A}_s} (N_\theta(\mathbf{s})[a])$, valid for $\forall \mathbf{s} \in \mathcal{S}$, and this policy is the initial policy in the next approximate policy iteration step, $i + 1$, continuing until π_n is obtained.

5 Experimental Setup

We next present the experimental setup employed to apply Deep Controlled Learning to three difficult inventory problems: lost sales inventory control, perishable inventory systems, and inventory systems with random lead times. Formulating the inventory systems under consideration within the MDP-EI framework $\mathcal{M} = \langle \mathcal{S}, \mathcal{A}, \mathcal{W}, \Xi, f, C, \alpha, \mathbf{s}_0 \rangle$ is straightforward and discussed in Appendix B. For each system, a base-stock policy is adopted as π_0 , see also the appendix.

The DCL algorithm is implemented in C++17; computations are performed on an AMD EPYC 7H12 processor with 128 hardware threads. Table 2 outlines the hyperparameters employed for all numerical experiments. We maintain consistency of the hyperparameters throughout the experiments to demonstrate the robustness of DCL across different models and their respective problem instances. Since exact policy iteration usually converges to near-optimal solutions within 3-6 steps

for stochastic models (Puterman, 2014), we opt for $n = 3$ approximate policy iteration steps. The sampling-related hyperparameters, N and L , are chosen to align with the discussion in §4.2. We select sufficiently high values for simulation parameters H and M to ensure accurate estimates of the action-value functions. We use a multi-layer perceptron as neural network architecture and use standard values for training hyperparameters, see Appendix A for details.

Sampling and Simulation		Neural Network Structure N_θ	
Horizon length:	$H = 40$	Number of layers:	4
Number of exogenous scenarios:	$M = 1000$	Number of neurons:	{ 256, 128, 128, 128 }
Number of samples:	$N = 5000$	Optimizer:	Adam
Length of the warm-up period:	$L = 100$	Mini-batch size:	$MiniBatchSize = 64$
Number of approximate policy iterations: $n = 3$			

Table 2: The hyperparameters used in the experiments.

6 Results

We compare the performance of Deep Controlled Learning with the top-performing heuristics of the three inventory management problems that we study. As a reflection of its widespread adoption and effectiveness, the base-stock policy also serves as a benchmark in the experiments. We aim to evaluate the potential of DCL in enhancing decision-making processes compared to the best heuristics in complex inventory systems. We then perform a quantitative analysis to specifically explore how the inclusion of Sequential Halving and Common Random Numbers impacts DCL performance.

6.1 Performance Evaluation on Inventory Problems

In the execution of our numerical experiments, we appropriate the problem instances previously utilized to gauge the efficacy of the best heuristics in their original papers. We refer readers to those benchmark papers for the theoretical and practical relevance of the selected instances. These instances include both situations where the computation of the optimal policy is feasible and more complex cases where the real benefit of approximation methods, including Deep Controlled Learning, becomes evident. For the remainder of our results, the instances will be referred to as "small instances" and "large instances", respectively.

We report optimality gaps for small instances and average costs per period or gap to the base stock policy for large instances. Optimality gaps are computed as $(v_\pi - v^*)/v^* \times 100\%$, where v_π denotes the average cost per time unit of the policy π , and v^* stands for the average cost per time unit of the optimal policy. Here, v_π and v^* are computed by explicitly solving the average-cost Bellman equations (Puterman, 2014). For large instances, we obtain unbiased estimators of the average costs per period through simulation. Each simulation is specifically comprised of 100 runs,

with each run spanning 10000 periods. The first run commences following a warm-up period of 100 periods, and the initial states for succeeding runs correspond to the final observed state of the preceding run. Results are statistically significant: the half-width of a 95% confidence interval is less than 1% of the corresponding cost value.

DCL generates three neural network policies by implementing three approximate policy iteration steps ($n = 3$). We report the performance of the best-performing neural network for each instance, which is typically (but not invariably) the third/last generation.

Lost sales inventory control

We first test the DCL algorithm on lost sales inventory control. Besides the base-stock policy (BSP), the benchmarks include the best-performing capped base-stock policy (CBS) and myopic-2-period policy (M-2), which provides better optimality gaps in some cases. We also report the results from a previous DRL application to such systems, the A3C algorithm by Gijbrenchts et al. (2022). We employ instances from the testbed proposed by Zipkin (2008) and Xin (2021). Specifically, we maintain a constant holding cost of $h = 1$ and adjust the penalty cost p to encompass the range $p = \{4, 9, 19, 39\}$. We apply two types of demand distributions, Poisson and geometric, both with a mean of five. For small instances, we set the lead time τ to $\{2, 3, 4\}$, while for large instances, we adopt lead times of $\tau = \{6, 8, 10\}$.

Table 3 delineates the optimality gaps for small instances and the average costs incurred by the policies for large instances. We report the optimality gaps of the benchmarks to one decimal place. The gaps for DCL are reported to two decimal places to retain a sense of the approximate magnitude of the optimality gap. For small cases, the table shows that DCL achieves a maximum optimality gap of 0.1%, indicating that the learned neural network successfully encapsulates the structure of the optimal policy to such an extent that it nearly matches its performance. Moreover, DCL outperforms other methods by achieving a gap at least ten times smaller. We also observe no clear pattern in the optimality gaps for DCL.

With regard to the average costs for larger cases, the table shows that DCL consistently yields lower costs than other methods for each instance, except for cases where $\tau = 10$, $p \in \{9, 19, 39\}$, and the demands are distributed according to a Poisson distribution. We posit that the number of samples ($N = 5000$) may be insufficient to cover the state space comprehensively for these instances. Therefore, we also train DCL with 20000 samples instead of 5000 while keeping other hyperparameters fixed and denote this model as DCL'. DCL' obtains a significant reduction in costs across all instances, thereby outperforming all heuristic results.

Computation times to apply DCL for individual instances vary between 100 and 300 seconds, while DCL' takes between 7 and 21 minutes. This demonstrates a significant improvement, particularly when contrasted with applying the A3C algorithm to inventory problems, which took

		Poisson						Geometric					
		Lead time τ						Lead time τ					
p	Policy	2	3	4	6	8	10	2	3	4	6	8	10
4	BSP	5.5%	8.2%	9.9%	5.51	5.72	5.86	4.5%	6.4%	7.8%	11.86	12.12	12.31
	CBS	0.2%	0.7%	1.5%	5.03	5.19	5.27	0.8%	0.4%	0.8%	10.91	10.96	10.98
	M-2	0.2%	0.8%	1.9%	5.05	5.20	5.31	0.5%	1.2%	1.7%	11.08	11.27	11.40
	A3C	3.2%	3.0%	6.7%	—	—	—	—	—	—	—	—	—
	DCL	0.00%	0.03%	0.04%	4.87	4.95	5.04	0.02%	0.02%	0.02%	10.75	10.82	10.91
	DCL'	0.00%	0.01%	0.03%	4.87	4.95	5.00	0.01%	0.01%	0.02%	10.75	10.82	10.87
9	BSP	3.7%	5.1%	6.4%	7.90	8.32	8.63	3.1%	4.6%	5.8%	18.53	19.18	19.68
	CBS	0.5%	1.4%	1.0%	7.26	7.55	7.77	0.8%	0.8%	0.9%	17.35	17.68	17.88
	M-2	0.2%	0.6%	1.2%	7.43	7.77	8.08	0.5%	1.1%	1.9%	17.75	18.39	18.89
	A3C	4.8%	3.1%	3.4%	—	—	—	—	—	—	—	—	—
	DCL	0.00%	0.01%	0.04%	7.23	7.52	7.85	0.02%	0.01%	0.01%	17.16	17.52	17.75
	DCL'	0.00%	0.00%	0.03%	7.22	7.49	7.68	0.01%	0.01%	0.01%	17.13	17.48	17.71
19	BSP	2.3%	2.9%	3.9%	10.20	10.90	11.48	2.0%	3.0%	3.9%	25.54	26.81	27.82
	CBS	0.8%	0.5%	0.7%	9.80	10.35	10.66	0.8%	1.0%	1.4%	24.49	25.38	25.98
	M-2	0.1%	0.4%	0.8%	9.85	10.53	11.09	0.3%	0.8%	1.4%	24.93	26.21	27.27
	DCL	0.01%	0.02%	0.06%	9.66	10.20	10.82	0.01%	0.01%	0.03%	24.20	25.10	25.81
	DCL'	0.00%	0.01%	0.02%	9.64	10.17	10.57	0.01%	0.01%	0.01%	24.19	25.09	25.73
39	BSP	0.9%	1.8%	2.5%	12.38	13.39	14.24	1.3%	2.0%	2.6%	32.69	34.47	36.25
	CBS	0.3%	0.4%	0.8%	12.08	12.94	13.71	0.3%	1.1%	1.4%	31.86	33.97	35.64
	M-2	0.1%	0.3%	0.4%	12.11	13.09	13.93	0.2%	0.5%	0.9%	32.12	34.12	35.82
	DCL	0.00%	0.04%	0.10%	11.97	12.82	14.22	0.01%	0.03%	0.03%	31.49	33.11	34.40
	DCL'	0.00%	0.01%	0.02%	11.94	12.81	13.48	0.01%	0.02%	0.02%	31.45	33.07	34.33

Table 3: Optimality gaps (for $\tau = \{2, 3, 4\}$) and average costs (for $\tau = \{6, 8, 10\}$) of selected policies on lost sales inventory control, with the best-performing policies for each problem *highlighted*. Results for A3C are reported where exact numerical results are available in the respective paper (see Gijbrecchts et al., 2022).

days due to the need for extensive hyperparameter tuning. (When assessing this computation time and comparing it to computation times reported by others, one should consider the capabilities of different computing machines regarding the number of threads and their computational power and the possible availability of accelerators (not available in our case).) We also find that the training of neural networks is consistently completed within 15 and 40 seconds for DCL and DCL', respectively. The remainder of the computation time can be largely attributed to the simulations. These are observed to consume more time when the lead time was longer and when the demand followed a geometric distribution. This is to be expected, as these conditions require evaluating a larger number of actions, leading to creating a greater number of exogenous scenarios because the total budget is $B_s = M|\mathcal{A}_s|$ for a state \mathbf{s} .

Considering all these results, it becomes clear that DCL sets new performance benchmarks for the well-established testbed of the canonical lost sales inventory control problem.

Perishable inventory systems

We next turn our attention to the performance of DCL on perishable inventory systems. The

benchmark policies for comparison include the base-stock policy and the BSP-low-EW policy by Haijema and Minner (2019). In order to evaluate the performance of these policies, we have selected a subset comprising 81 diverse instances from the extensive testbed of 11177 instances utilized by Haijema and Minner (2019). Our selection focuses on those settings that require non-trivial policies, ensuring a robust and comprehensive assessment. The holding cost is set at $h = 0$, the penalty cost at $p = 100$, and the waste cost at $w = 100$. We maintain a constant total mean demand per period of $\mu = 4$, while the coefficient of variation cvr ranges between $\{1.0, 1.5, 2.0\}$. On average, a fraction f of demand is fulfilled by the First-In-First-Out (FIFO) issuing policy, with the remaining fraction $1 - f$ satisfied by the Last-In-First-Out (LIFO) policy. This is modeled through two discrete demand distributions, fitted using the method proposed by Adan et al. (1995). In the experiments, the probability f varies between $f = \{1.0, 0.5, 0.0\}$. We also set the product lifetime $m_l = \{3, 4, 5\}$ and order lead time $\tau = \{0, 1, 2\}$. Small instances correspond to cases where $m_l + \tau \leq 5$ for $f = 0$ and $f = 1$, and $m_l + \tau < 4$ for $f = 0.5$. The difference arises from the fact that $f = 0.5$ requires two fitted demand distributions, which increases the possible state transitions. Large instances correspond to the remaining cases.

	All Instances			Small Instances			Large Instances	
	Avg. Cost	Avg. BSP gap		Avg. Opt. gap			Avg. BSP gap	
Instances	BSP	BSP-low-EW	DCL	BSP	BSP-low-EW	DCL	BSP-low-EW	DCL
<i>All</i>	75.3	-4.6%	-8.7%	9.7%	4.1%	0.03%	-4.3%	-9.0%
$m_l = 3$	99.7	-6.5%	-8.7%	9.1%	2.6%	0.02%	-11.7%	-13.2%
$m_l = 4$	71.8	-4.4%	-8.5%	9.2%	5.3%	0.04%	-5.6%	-9.0%
$m_l = 5$	54.4	-3.0%	-8.8%	13.0%	7.5%	0.04%	-2.6%	-8.3%
$\tau = 0$	57.4	-3.2%	-7.6%	9.1%	4.9%	0.02%	-0.5%	-6.0%
$\tau = 1$	77.5	-3.9%	-7.7%	8.8%	3.9%	0.03%	-3.2%	-7.3%
$\tau = 2$	90.9	-6.8%	-10.7%	13.9%	1.6%	0.06%	-5.6%	-10.3%
$cvr = 1.0$	37.2	-4.5%	-9.4%	10.9%	5.0%	0.03%	-3.8%	-9.5%
$cvr = 1.5$	74.0	-4.9%	-8.8%	9.9%	4.3%	0.05%	-4.8%	-9.1%
$cvr = 2.0$	114.6	-4.5%	-7.8%	8.2%	3.1%	0.02%	-4.4%	-8.4%
$f = 1.0$	47.9	-3.7%	-6.8%	6.3%	2.8%	0.02%	-4.6%	-8.8%
$f = 0.5$	74.1	-3.7%	-6.9%	5.1%	3.0%	0.04%	-4.5%	-7.9%
$f = 0.0$	103.8	-6.6%	-12.4%	15.3%	6.0%	0.04%	-3.7%	-11.3%

Table 4: Average costs of BSP, the optimality gaps, and the difference in average costs between BSP and DCL - BSP-low-EW.

In line with the results in Haijema and Minner (2019), we average the results according to identical experimental parameters. Table 4 provides an overview of these findings, reporting the average cost of the base-stock policy, the optimality gaps of the three policies for small instances, and the relative improvement of the DCL and BSP-low-EW policies over the base-stock policy for large instances and also for all instances. The relative improvement of DCL over BSP can be calculated by the formula $(v_{\pi_{DCL}} - v_{\pi_{BSP}})/v_{\pi_{BSP}} \times 100\%$, with $v_{\pi_{DCL}}$ denoting average cost of DCL

and $v_{\pi_{BSP}}$ denoting average cost of BSP, respectively.

We observe that DCL substantially outperforms both policies both for small and large instances. For small instances, it achieves a markedly lower average optimality gap (0.03%) and consistently delivers robust performance across different settings, including various issuing policies. For large instances, DCL performs considerably better than BSP as well as BSP-low-EW. We further note that the relative cost improvement of DCL over BSP tends to increase with longer lead times and with an increase in demand met through the LIFO issuing policy when averaged over all instances.

Similar to our lost sales inventory control experiments, the computation times to apply DCL for individual instances range between 150 – 200 seconds and tend to increase as $m_l + \tau$ expands.

Inventory systems with random lead times

Finally, we evaluate the performance of DCL on inventory systems with random lead times. Our benchmark policies are the base-stock policy and the generalized base-stock policy (GBS) (Stolyar and Wang, 2022). We set the maximum order quantity at a decision epoch to $m = 6$, as GBS policy is likely to order less than this number in the selected problem instances.

We consider the instances adopted by Stolyar and Wang (2022) for numerical experiments, which comprise cases with two distinct lead time distributions: exponential (small instances) and uniform (large instances). When the lead time is exponentially distributed, information regarding elapsed time for pending orders becomes irrelevant due to the memoryless nature of the exponential distribution. As a result, a state \mathbf{s} corresponds to a vector in \mathbb{R}^2 that represents the inventory level ($\mathbf{s}[1]$) and the inventory in the pipeline ($\mathbf{s}[2]$), omitting the vector \mathbf{x} . This reduction facilitates the computation of the optimal policy. For both lead time distribution cases, we maintain the holding cost h , and the backorder cost b at a constant value of 1, and vary the ratio μ/β which takes values in $\{2, 10, 20\}$, where μ represents the mean demand rate and β denotes the mean lead time. Lastly, we replicate the sensitivity analysis performed by Stolyar and Wang (2022) for the exponential distribution case. We keep $\mu/\beta = 20$ constant and alternate one of the holding cost h , or the backorder cost b within the range $\{3, 6, 9\}$ while maintaining the other at 1.

	μ/β	2	10	20	20	20	20	20	20	20
	h	1	1	1	9	6	3	1	1	1
	b	1	1	1	1	1	1	3	6	9
Exponential lead time	BSP	1.08	2.50	3.54	7.44	6.74	5.52	5.79	7.34	8.16
	GBS	1.00	2.01	2.66	5.62	5.22	4.17	4.18	5.14	5.58
	DCL	0.95	1.87	2.46	5.50	4.90	3.95	3.93	4.92	5.42
	Optimal	0.95	1.87	2.45						
Uniform lead time	BSP	1.08	2.50	3.54						
	GBS	1.06	2.29	3.13						
	DCL	1.02	2.14	2.90						

Table 5: Average costs of policies when lead times are exponentially or uniformly distributed.

Table 5 reports the average costs of the policies across the selected instances, showcasing the dominant performance of DCL. In cases of exponential lead time, we observe that DCL nearly mirrors the average costs of the optimal policy, suggesting the efficiency of DCL in grasping the structure of the optimal policy under such settings. For instances with uniform lead time, although DCL retains its superiority over GBS, the difference in their performance narrows. The gap between BSP and GBS likewise contracts. This contraction might be ascribed to the inherent nature of the uniform distribution, which has an increasing hazard rate, potentially negatively affecting the development of proficient policies (Stolyar and Wang, 2022).

The computation times for applying DCL to individual instances vary between 150–300 seconds.

6.2 Impact of SH with CRN on Performance Improvements

The numerical results reveal that DCL is a powerful framework for addressing intractable inventory management problems, outdoing the top-performing heuristics. Next, we focus on quantifying the benefits of incorporating Sequential Halving with Common Random Numbers in the algorithm’s simulation phase. To investigate the impact of these techniques on the efficiency of DCL, we rerun the numerical experiments for the three inventory problems. This time, however, we employ DCL without incorporating them. Specifically, in the process of determining the simulation-based action $\hat{\pi}^+(\mathbf{s})$ for any given state \mathbf{s} , DCL distributes the total exogenous scenario budget uniformly among each applicable action $a \in \mathcal{A}_{\mathbf{s}}$ – a methodology referred to as uniform allocation – and simultaneously alternates the scenarios among the actions, which implies the absence of Common Random Numbers. This variant of the DCL algorithm is referred to as DCL₀.

Table 6 provides a comprehensive overview of the optimality gaps (for small instances) and the relative improvements of the policies over the base-stock policy regarding average costs (BSP gap for large instances and for all instances). These values represent averages across all respective instances for each inventory setting, with our consideration focusing on DCL, DCL₀, and π_{heur} , the latter being the best heuristic for each corresponding inventory problem.

	Lost Sales			Perishable			Random Lead Times		
	DCL	DCL ₀	π_{heur}	DCL	DCL ₀	π_{heur}	DCL	DCL ₀	π_{heur}
Optimality gap	0.02%	1.2%	0.8%	0.03%	0.8%	4.1%	0.1%	0.8%	7.1%
BSP gap (large instances)	-6.2%	2.8%	-5.4%	-9.0%	-7.8%	-4.3%	-12.7%	-12.0%	-7.3%
BSP gap (all instances)	-5.6%	-1.3%	-4.8%	-8.7%	-7.8%	-4.6%	-23.9%	-23.1%	-19.5%

Table 6: Performance comparison of DCL, DCL₀ and the best heuristics.

The results in Table 6 yield two salient observations. Initially, DCL₀ demonstrates remarkable performance, surpassing the best heuristic benchmarks on perishable inventory systems and inventory systems with stochastic lead times. It also exhibits competitive performance relative to the base-stock policy in lost sales inventory control. Intriguingly, DCL₀ manages to secure optimality

gaps around 1%, which, when placed in comparison with the prior deep reinforcement learning application, A3C (Gijbrecchts et al., 2022), represents a significant enhancement. To offer perspective, A3C records optimality gaps within 3 – 6% for lost sales inventory control. This justifies our initial motivation that inventory management problems may require evaluating states under multiple exogenous scenarios for subsequent policy updates. As a result, even without advanced techniques in the simulation part of DCL, it is possible to obtain superior results.

Subsequently, a second observation emerges as critical: the integration of Sequential Halving with Common Random Numbers into the DCL algorithm yields a tangible amplification in performance, culminating in optimality gaps that are superior by more than an order of magnitude, all the while operating within the same simulation resource constraints ($M = 1000$). This duality in observations underscores both our initial motivation to design a DRL algorithm specifically for MDP-EI and the pivotal role of the simulation techniques in bolstering its efficiency.

These results prompt an important follow-up question: how many additional simulation resources would be required for DCL_0 to match DCL’s performance? To investigate this, we conduct a series of simulations by adjusting the number of exogenous scenarios (M) from the set $\{100, 500, 1000, 2000, 5000, 10000, 20000\}$, while maintaining other hyperparameters constant. (We note that the total budget B_s of exogenous scenarios for a sampled state \mathbf{s} is $B_s = \mathcal{A}_s |M|$.) Since the purpose of simulations is to identify the simulation-based action $\hat{\pi}^+(\mathbf{s})$ that closely approximates or matches the optimal action $\pi^+(\mathbf{s})$, we examine how varying resource allocation strategies impact the accuracy of determining simulation-based actions. To this end, we evaluate four simulation strategies: Sequential Halving with Common Random Numbers (DCL), Sequential Halving without CRN, Uniform Allocation with CRN, and Uniform Allocation without CRN (DCL_0).

To obtain rigorous analysis, we select six diverse ”small” instances from the studied inventory management problems (from lost sales inventory control with 1-) Poisson demand, $\tau = 3$, $p = 39$, 2-) Poisson demand, $\tau = 4$, $p = 19$ and 3-) geometric demand, $\tau = 3$, $p = 19$; from perishable inventory systems with 4-) $m_l = 4$, $\tau = 1$, $f = 1.0$, $cvr = 1.5$, 5-) $m_l = 4$, $\tau = 1$, $f = 0.0$, $cvr = 1.5$ and 6-) $m_l = 3$, $\tau = 1$, $f = 0.5$, $cvr = 1.5$), where we can computationally find the optimal action $\pi^+(\mathbf{s})$ for a state \mathbf{s} before following the policy π . Consequently, we can analyze the performance of the selected simulation algorithms by measuring the accuracy (correct classification %) of how well they can find $\hat{\pi}^+(\mathbf{s})$ such that $\hat{\pi}^+(\mathbf{s}) = \pi^+(\mathbf{s})$ for the sampled states.

Figure 2 provides the average results of these experiments, where $M = 1000$ denotes the setting we use to obtain numerical results. We observe that the main performance gain is obtained by the inclusion of Common Random Numbers when generating exogenous scenarios, hinting at a huge variance reduction when comparing the estimated expected costs of two actions. Moreover, Sequential Halving provides up to 10% better correct classification in pursuing the optimal action when equipped with CRN. Notably, without CRN and SH, the simulation process suffers from

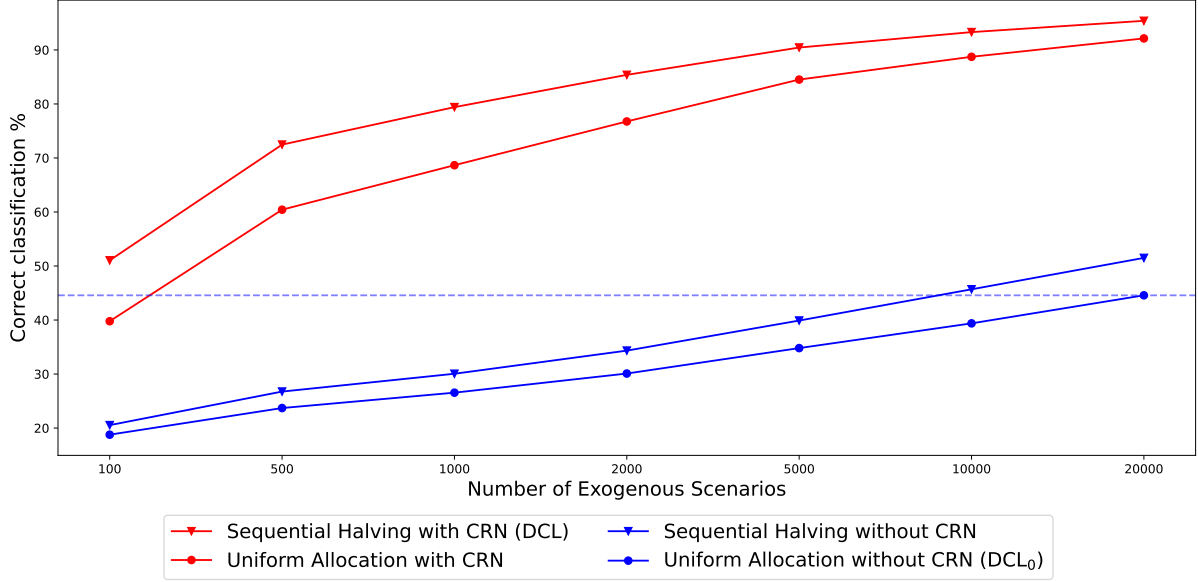


Figure 2: Correct classification % of simulation strategies in determining the optimal actions.

variance and cannot allocate resources to promising actions. To illustrate this claim, the dashed horizontal line in Figure 2 shows that DCL_0 would need to generate exogenous scenarios at a volume more than a hundred times higher to match the performance of DCL in finding the simulation-based actions.

7 Conclusion

The current body of literature acknowledges the potential of deep reinforcement learning (DRL) algorithms in addressing complex inventory management problems (Boute et al., 2022). While the initial outcomes have been encouraging, there remains a degree of uncertainty regarding the practical application of such algorithms, particularly their ability to supersede established heuristics.

In this research, we bridge this gap by enhancing the applicability and performance of DRL in the challenging domain of inventory management. We develop a framework that surpasses the limitations of existing DRL applications, with a particular focus on the unique challenges presented by inventory management scenarios.

In particular, we introduce the Deep Controlled Learning (DCL) algorithm, tailored to address inventory-specific challenges. DCL outperformed top heuristics in areas like lost sales control, perishable systems, and random lead-time scenarios. The techniques used, notably Sequential Halving with Common Random Numbers (referenced in §6.2), enhance simulation efficiency, elevating DCL’s performance. With consistent hyperparameters throughout our experiments, DCL’s robustness is underscored. These results substantiate our initial hypothesis, suggesting that DRL indeed holds promise for inventory management problems but requires tailored algorithms to meet their unique

requirements.

Acknowledgements

Tarkan Temizöz conducted his research in the project DynaPlex: Deep Reinforcement Learning for Data-Driven Logistics, made possible by TKI Dinalog and the Topsector Logistics and funded by the Ministry of Economic Affairs and Climate Policy. We acknowledge the support of the SURF Cooperative using grant no. EINF-5192.

References

- Adan, I., van Eenige, M., and Resing, J. (1995). Fitting discrete distributions on the first two moments. *Probability in the Engineering and Informational Sciences*, 9(4):623–632.
- Ang, M., Sigman, K., Song, J.-S., and Zhang, H. (2017). Closed-form approximations for optimal (r, q) and (s, t) policies in a parallel processing environment. *Operations Research*, 65(5):1414–1428.
- Bijvank, M. and Vis, I. F. (2011). Lost-sales inventory theory: A review. *European Journal of Operational Research*, 215(1):1–13.
- Boute, R. N., Gijsbrechts, J., van Jaarsveld, W., and Vanvuchelen, N. (2022). Deep reinforcement learning for inventory control: A roadmap. *European Journal of Operational Research*, 298(2):401–412.
- Bradley, J. R. and Robinson, L. W. (2005). Improved base-stock approximations for independent stochastic lead times with order crossover. *Manufacturing & Service Operations Management*, 7(4):319–329.
- Broekmeulen, R. A. and van Donselaar, K. H. (2009). A heuristic to manage perishable inventory with batch ordering, positive lead-times, and time-varying demand. *Computers & Operations Research*, 36(11):3013–3018.
- Bu, J., Gong, X., and Chao, X. (2023). Asymptotic optimality of base-stock policies for perishable inventory systems. *Management Science*, 69(2):846–864.
- Bubeck, S. and Cesa-Bianchi, N. (2012). Regret analysis of stochastic and nonstochastic multi-armed bandit problems. *Foundations and Trends® in Machine Learning*, 5(1):1–122.
- Cachon, G. P., Girotra, K., and Netessine, S. (2020). Interesting, important, and impactful operations management. *Manufacturing & Service Operations Management*, 22(1):214–222.

- Chao, X., Gong, X., Shi, C., Yang, C., Zhang, H., and Zhou, S. X. (2018). Approximation algorithms for capacitated perishable inventory systems with positive lead times. *Management Science*, 64(11):5038–5061.
- Chen, W., Dawande, M., and Janakiraman, G. (2014). Fixed-dimensional stochastic dynamic programs: An approximation scheme and an inventory application. *Operations Research*, 62(1):81–103.
- Clark, A. and Scarf, H. (1960). Optimal policies for a multi-echelon inventory problem. *Management Science*, 6(4):475–490.
- Cohen, M. and Pekelman, D. (1978). Lifo inventory systems. *Management Science*, 24(11):1150–1162.
- Danihelka, I., Guez, A., Schrittwieser, J., and Silver, D. (2022). Policy improvement by planning with gumbel. In *International Conference on Learning Representations*.
- De Moor, B. J., Gijsbrechts, J., and Boute, R. N. (2022). Reward shaping to improve the performance of deep reinforcement learning in perishable inventory management. *European Journal of Operational Research*, 301(2):535–545.
- Dietterich, T. G., Trimponias, G., and Chen, Z. (2018). Discovering and removing exogenous state variables and rewards for reinforcement learning. In *International Conference on Machine Learning*, pages 1262–1270. PMLR.
- Disney, S. M., Maltz, A., Wang, X., and Warburton, R. D. (2016). Inventory management for stochastic lead times with order crossovers. *European Journal of Operational Research*, 248(2):473–486.
- Ernst, D., Geurts, P., and Wehenkel, L. (2005). Tree-based batch mode reinforcement learning. *Journal of Machine Learning Research*, 6(18):503–556.
- Fabiano, N. and Cazenave, T. (2022). Sequential halving using scores. In Browne, C., Kishimoto, A., and Schaeffer, J., editors, *Advances in Computer Games*, pages 41–52, Cham. Springer International Publishing.
- Federgruen, A. and Zipkin, P. (1984). Approximations of dynamic, multilocation production and inventory problems. *Management Science*, 30(1):69–84.
- Geevers, K., van Hezewijk, L., and Mes, M. R. (2023). Multi-echelon inventory optimization using deep reinforcement learning. Available at SSRN: <https://ssrn.com/abstract=4227665> or <http://dx.doi.org/10.2139/ssrn.4227665>.

- Gijsbrechts, J., Boute, R. N., Van Mieghem, J. A., and Zhang, D. J. (2022). Can deep reinforcement learning improve inventory management? performance on lost sales, dual-sourcing, and multi-echelon problems. *Manufacturing & Service Operations Management*, 24(3):1349–1368.
- Goldberg, D. A., Katz-Rogozhnikov, D. A., Lu, Y., Sharma, M., and Squillante, M. S. (2016). Asymptotic optimality of constant-order policies for lost sales inventory models with large lead times. *Mathematics of Operations Research*, 41(3):898–913.
- Goodfellow, I., Bengio, Y., and Courville, A. (2016). *Deep Learning*. MIT Press. <http://www.deeplearningbook.org>.
- Haijema, R. and Minner, S. (2019). Improved ordering of perishables: The value of stock-age information. *International Journal of Production Economics*, 209:316–324. The Proceedings of the 19th International Symposium on Inventories.
- Hong, L. J., Fan, W., and Luo, J. (2021). Review on ranking and selection: A new perspective. *Frontiers of Engineering Management*, 8:321–343.
- Huh, W. T., Janakiraman, G., Muckstadt, J. A., and Rusmevichientong, P. (2009). Asymptotic optimality of order-up-to policies in lost sales inventory systems. *Management Science*, 55(3):404–420.
- Johansen, S. and Thorstenson, A. (2008). Pure and restricted base-stock policies for the lost-sales inventory system with periodic review and constant lead times. 15th International Symposium on Inventories ; Conference date: 22-08-2008 Through 26-08-2008.
- Karaesmen, I., Scheller-Wolf, A., and Deniz, B. (2011). Managing perishable and aging inventories: Review and future research directions. In Kempf, K., Keskinocak, P., and Uzsoy, R., editors, *Planning Production and Inventories in the Extended Enterprise*, volume 151 of *International Series in Operations Research & Management Science*, pages 393–436. Springer, New York.
- Karnin, Z., Koren, T., and Somekh, O. (2013). Almost optimal exploration in multi-armed bandits. In Dasgupta, S. and McAllester, D., editors, *Proceedings of the 30th International Conference on Machine Learning*, volume 28 of *Proceedings of Machine Learning Research*, pages 1238–1246, Atlanta, Georgia, USA. PMLR.
- Kingma, D. P. and Ba, J. (2014). Adam: A method for stochastic optimization. *arXiv preprint arXiv:1412.6980*.
- Lagoudakis, M. G. and Parr, R. (2003). Reinforcement learning as classification: Leveraging modern classifiers. In *Proceedings of the 20th International Conference on Machine Learning (ICML-03)*, pages 424–431.

- Law, A. M. and Kelton, W. D. (2000). *Simulation Modeling and Analysis*. McGraw-Hill, Boston, MA.
- Lazaric, A., Ghavamzadeh, M., and Munos, R. (2016). Analysis of classification-based policy iteration algorithms. *Journal of Machine Learning Research*, 17(19):1–30.
- Mao, H., Venkatakrisnan, S. B., Schwarzkopf, M., and Alizadeh, M. (2019). Variance reduction for reinforcement learning in input-driven environments. In *International Conference on Learning Representations*.
- Minner, S. and Transchel, S. (2010). Periodic review inventory-control for perishable products under service-level constraints. *OR Spectrum*, 32:979–996.
- Mnih, V., Badia, A. P., Mirza, M., Graves, A., Lillicrap, T., Harley, T., Silver, D., and Kavukcuoglu, K. (2016). Asynchronous methods for deep reinforcement learning. In *International conference on machine learning*, pages 1928–1937.
- Mnih, V., Kavukcuoglu, K., Silver, D., Rusu, A. A., Veness, J., Bellemare, M. G., Graves, A., Riedmiller, M., Fidjeland, A. K., Ostrovski, G., et al. (2015). Human-level control through deep reinforcement learning. *nature*, 518(7540):529–533.
- Morton, K. (1969). Bounds on the solution of the lagged optimal inventory equation with no demand backlogging and proportional costs. *SIAM Review*, 11(4):572–596.
- Morton, K. (1971). The near-myopic nature of the lagged-proportional-cost inventory problem with lost sales. *Operations Research*, 19(7):1708–1716.
- Muthuraman, K., Seshadri, S., and Wu, Q. (2015). Inventory management with stochastic lead times. *Mathematics of Operations Research*, 40(2):302–327.
- Nahmias, S. (1975a). A comparison of alternative approximations for ordering perishable inventory. *Information Systems and Operational Research*, 13(2):175–184.
- Nahmias, S. (1975b). Optimal ordering policies for perishable inventory—ii. *Operations Research*, 23(4):735–749.
- Nahmias, S. (2011). *Perishable Inventory Systems*. International Series in Operations Research & Management Science. Springer, New York.
- Oroojlooyjadid, A., Nazari, M., Snyder, L. V., and Takáč, M. (2021). A deep q-network for the beer game: Deep reinforcement learning for inventory optimization. *Manufacturing & Service Operations Management*, 24(1):285–304.

- Paszke, A., Gross, S., Massa, F., Lerer, A., Bradbury, J., Chanan, G., Killeen, T., Lin, Z., Gimelshein, N., Antiga, L., Desmaison, A., Kopf, A., Yang, E., DeVito, Z., Raison, M., Tejani, A., Chilamkurthy, S., Steiner, B., Fang, L., Bai, J., and Chintala, S. (2019). Pytorch: An imperative style, high-performance deep learning library.
- Powell, W. (2020). *Reinforcement Learning and Stochastic Optimization: A unified framework for sequential decisions*. Wiley-Interscience.
- Powell, W. B. (2011). *Approximate Dynamic Programming: Solving the Curses of Dimensionality*. Wiley, Hoboken, NJ.
- Powell, W. B. (2019). A unified framework for stochastic optimization. *European Journal of Operational Research*, 275(3):795–821.
- Puterman, M. L. (2014). *Markov decision processes: discrete stochastic dynamic programming*. John Wiley & Sons.
- Schulman, J., Wolski, F., Dhariwal, P., Radford, A., and Klimov, O. (2017). Proximal policy optimization algorithms. *arXiv preprint arXiv:1707.06347*.
- Silver, D., Hubert, T., Schrittwieser, J., Antonoglou, I., Lai, M., Guez, A., Lanctot, M., Sifre, L., Kumaran, D., Graepel, T., et al. (2018). A general reinforcement learning algorithm that masters chess, shogi, and go through self-play. *Science*, 362(6419):1140–1144.
- Silver, E. A., Pyke, D. F., and Peterson, R. (1998). *Inventory Management and Production Planning and Scheduling*. John Wiley & Sons.
- Stolyar, A. L. and Wang, Q. (2022). Exploiting random lead times for significant inventory cost savings. *Operations Research*, 70(4):2496–2516.
- Sun, P., Wang, K., and Zipkin, P. (2016). Quadratic approximation of cost functions in lost sales and perishable inventory control problems. Working paper, Fuqua School of Business, Duke University, Durham, NC.
- Sutton, R. S. and Barto, A. G. (2018). *Reinforcement Learning: An Introduction*. MIT Press, 2nd edition.
- Tesauro, G. and Galperin, G. (1996). On-line policy improvement using monte-carlo search. In Mozer, M., Jordan, M., and Petsche, T., editors, *Advances in Neural Information Processing Systems*, volume 9. MIT Press.

- Trimponias, G. and Dietterich, T. G. (2023). Reinforcement learning with exogenous states and rewards. *arXiv preprint arXiv:2303.12957*.
- van Hezewijk, L., Dellaert, N. P., van Woensel, T., and Gademann, A. J. R. M. (2023). Using the proximal policy optimisation algorithm for solving the stochastic capacitated lot sizing problem. *International Journal of Production Research*, 61(6):1955–1978.
- Van Houtum, G.-J. and Kranenburg, B. (2015). *Spare parts inventory control under system availability constraints*, volume 227. Springer.
- Vanvuchelen, N., Gijsbrechts, J., and Boute, R. (2020). Use of Proximal Policy Optimization for the Joint Replenishment Problem. *Computers in Industry*, 119:103239.
- Xin, L. (2021). Technical note—understanding the performance of capped base-stock policies in lost-sales inventory models. *Operations Research*, 69(1):61–70.
- Xin, L. and Goldberg, D. A. (2016). Optimality gap of constant-order policies decays exponentially in the lead time for lost sales models. *Operations Research*, 64(6):1556–1565.
- Zipkin, P. (2008). Old and new methods for lost-sales inventory systems. *Operations Research*, 56(5):1256–1263.
- Zipkin, P. H. (2000). *Foundations of Inventory Management*. McGraw-Hill, Boston.

A Training neural network classifiers

The training of the neural network and the subsequent update of parameters within Deep Controlled Learning framework are grounded in a standard set of strategies, as delineated in the *Deep Learning* book (Goodfellow et al., 2016), and further detailed in Algorithm 4. These techniques are widely applied across various classification tasks while there exist opportunities for further refinement.

Algorithm 4 Classifier

```

1: Input:  $N_\theta, \mathcal{K}$ 
2: Initialize: Neural networks parameters:  $\theta$ 
3: for  $e = 1, \dots, MaxEpoch$  do
4:   Shuffle  $\mathcal{K}$  and construct  $\mathcal{K}^{Tr}$  and  $\mathcal{K}^{Val}$ 
5:   Construct mini-batches  $\mathcal{K}_{mb}^{Tr}; \forall \mathcal{K}_{mb}^{Tr} \subset \mathcal{K}^{Tr}, |\mathcal{K}_{mb}^{Tr}| = MiniBatchSize$ 
6:   for all  $\mathcal{K}_{mb}^{Tr} \subset \mathcal{K}^{Tr}$  do
7:     Compute  $\mathcal{L}_\theta(\mathcal{K}_{mb}^{Tr})$  by (13)
8:      $\theta = Optimizer(\theta, \mathcal{L}_\theta(\mathcal{K}_{mb}^{Tr}))$ , (see Goodfellow et al., 2016)
9:   end for
10:  Compute  $\mathcal{L}_\theta(\mathcal{K}^{Val})$  by (13)
11:  if  $StoppingCondition(\mathcal{L}_\theta(\mathcal{K}^{Val}))$ , (see Goodfellow et al., 2016) then
12:    break
13:  end if
14: end for
15:  $\pi_\theta(\mathbf{s}) = \arg \max_{a \in \mathcal{A}_\mathbf{s}} (N_\theta(\mathbf{s})[a]), \forall \mathbf{s} \in \mathcal{S}$ 
16: Output:  $\pi_\theta$ 

```

In detail, DCL takes a dataset and a *neural network structure* N_θ , encapsulating the network architecture, training details, and hyperparameters, as inputs. It employs gradient-descent-based optimization across multiple epochs, each of which is defined as a complete cycle through the entire dataset with corresponding adjustments to the model’s parameters to minimize the loss function. The dataset undergoes random shuffling and partitioning for every epoch into a training set \mathcal{K}^{Tr} and a validation set \mathcal{K}^{Val} . While the training set provides the platform for the neural network classifier to approximate the simulation-based policy, the validation set serves as a benchmark for the evaluation of the policy’s performance and generalization capability. Furthermore, the training set is subdivided into *mini-batches* of fixed size, each facilitating a step of training to expedite the learning process and optimize computational resources. The model’s parameters undergo updates via gradient descent, anchored by the loss function computed from each mini-batch.

The loss for a given sample $(\mathbf{s}, \hat{\pi}^+(\mathbf{s}))$ is defined using the *cross-entropy* loss, a common loss function employed in classification tasks which gauges the discrepancy between the softmax of the neural network’s output (predicted probabilities for actions) for state \mathbf{s} (where actions $a \notin \mathcal{A}_\mathbf{s}$ are masked) and the simulation-based action $\hat{\pi}^+(\mathbf{s})$. The loss function for a sample $(\mathbf{s}, \hat{\pi}^+(\mathbf{s}))$ can be

thus formulated as:

$$l(\mathbf{s}, \hat{\pi}^+(\mathbf{s})|\theta) := -\log \frac{\exp(N_\theta(\mathbf{s})[\hat{\pi}^+(\mathbf{s})])}{\sum_{a' \in \mathcal{A}_s} \exp(N_\theta(\mathbf{s})[a'])}, \quad (12)$$

where $N_\theta(\mathbf{s})[a]$ represents the neural network’s predicted probability for action a . Subsequently, the average loss function over a dataset \mathcal{K} can be defined as:

$$\mathcal{L}_\theta(\mathcal{K}) := \frac{1}{|\mathcal{K}|} \sum_{(\mathbf{s}, \hat{\pi}^+(\mathbf{s})) \in \mathcal{K}} l(\mathbf{s}, \hat{\pi}^+(\mathbf{s})|\theta). \quad (13)$$

During each epoch, an *optimizer* iteratively updates the parameters θ with the aim of minimizing the average loss function, utilizing gradient-descent-based optimization (Line 8 in Algorithm 4). As a result, the divergence between the simulation-based policy and the predicted probabilities from the neural network diminishes. This occurs because the neural network is trained to assign high probabilities to each state’s simulation-based action, which leads to a more accurate approximation. Concurrently, the average loss function over the validation set \mathcal{K}^{Val} is calculated to monitor the neural network’s generalization ability. This iterative process of parameter updating persists until either the maximum number of epochs is reached, or a pre-determined stopping condition is met, the latter designed to ensure the neural network’s effective generalization.

Finally, the neural network policy is defined as $\pi_\theta(\mathbf{s}) = \arg \max_{a \in \mathcal{A}_s} (N_\theta(\mathbf{s})[a])$, valid for $\forall \mathbf{s} \in \mathcal{S}$, upon the completion of training.

Implementation in numerical experiments

Our implementation of neural networks in numerical experiments leverages the PyTorch framework’s C++ front-end for neural network training and inference (Paszke et al., 2019). The chosen architecture is a multi-layer perceptron utilized to approximate the policies. We stipulate a maximum of 1000 epochs for the training process. During each epoch, a random selection of 95% of the samples in \mathcal{K} forms the training set \mathcal{K}^{Tr} , with the residual samples constituting the validation set \mathcal{K}^{Val} . The parameters of the neural network are updated by minimizing the average loss (13) over the samples in mini-batches, each consisting of 64 samples, employing the Adam Optimizer (refer to Kingma and Ba, 2014). As suggested in the associated paper, we retain its default hyperparameters, including the learning rate. The Adam Optimizer is recognized for its proficiency in addressing many gradient-descent-based optimization problems (Goodfellow et al., 2016). As for the termination criterion, we employ an early stopping strategy, which serves as a potent regularization technique by preventing overfitting by terminating the training when the validation set performance ceases to improve. Specifically, after every 5 epochs, the network parameters θ are checkpointed. The algorithm ceases when the best test loss fails to improve over 20 consecutive epochs and returns the checkpointed network parameters corresponding to the best test loss

achieved up to that point. Our empirical observations suggest that the training process generally concludes within 100 epochs. For more insights into this implementation strategy, the readers are referred to Goodfellow et al. (2016).

B Formulating the inventory models as MDP-EI

For all problems, we consider a single product and adopt a finite action set $\mathcal{A} = \{0, 1, \dots, m\}$, where actions represent the amount ordered by the decision-maker. Consistent with the literature, we aim to minimize the average cost over an infinite horizon and hence $\alpha = 1$. The algorithm is rather insensitive to \mathbf{s}_0 ; we let the initial state correspond to having no stock on hand or in the pipeline.

Lost sales inventory control

We direct readers to §3 of the main paper for the MDP-EI formulation of the lost sales inventory control problem. It remains to discuss π_0 , $|\mathcal{A}| = m$, and $\mathcal{A}_{\mathbf{s}}$ for each state. Let I_{\max} denote the newsvendor fractile for cumulative demand over τ periods, which bounds the optimal inventory position (see Zipkin, 2008). Then π_0 will be a base-stock policy with base-stock level I_{\max} , and $\mathcal{A}_{\mathbf{s}}$ for state \mathbf{s} is constructed to ensure that the inventory position does not exceed I_{\max} . The maximum order quantity m corresponds to the single-period newsvendor fractile bound (see Zipkin, 2008).

Perishable inventory systems

We consider a periodic review perishable inventory system of a product possessing a maximum life of m_l periods and having a lead time $\tau \geq 0$, following Haijema and Minner (2019). Accordingly, the exogenous input encapsulates two stochastic variables $\xi = (\xi^{FIFO}, \xi^{LIFO})$, which represent the number of demands observed at the period's end under FIFO and LIFO issuance policies, respectively.

For state representation, we follow Bu et al. (2023): states \mathbf{s} are depicted as vectors in $\mathbb{R}^{m_l + \max(\tau-1, 0)}$, where $\mathbf{s}[i]$, for $i = 1, \dots, m_l$, denotes the inventory level of items with at most i period(s) life-time remaining. Thus $\mathbf{s}[m_l]$ corresponds to the total on-hand inventory at the period's outset. If the lead time $\tau > 1$, $\mathbf{s}[i]$, for $i = m_l + 1, \dots, m_l + \tau - 1$, denotes $\mathbf{s}[m_l]$ plus the amounts of pipeline inventory arriving in the next $i - m_l$ periods. State transitions are a bit involved; we refer to Bu et al. (2023) for a complete description. We denote the cost function as $C(\mathbf{s}, a, \xi) = wn_{\text{perish}} + h(\mathbf{s}[m_l] - d - n_{\text{perish}})^+ + p(d - \mathbf{s}[m_l])^+$, where n_{perish} denotes the number of perished units at a period's end, w denotes the waste cost of a unit perished at the period's end, h denotes holding cost, p denotes penalty cost, and $d = \xi^{FIFO} + \xi^{LIFO}$ represents the total demand.

We will employ the base-stock policy as the initial policy π_0 . We limit the maximum inventory position by $I_{\max} = m$, equating these parameters to the newsvendor solution required to cater to demand over $\tau + m_l$ periods, i.e., when the inventory on hand and in the pipeline have turned into waste (see Haijema and Minner, 2019).

Inventory systems with random lead times

We consider a continuous review inventory system with independent, identically distributed replenishment lead times with order-crossing and backlogged unsatisfied demands. Crucially, the decision-maker lacks access to order arrival times for orders in the pipeline. To simplify the exposition, we assume a fixed maximum for the allowable pipeline inventory, denoted as il_{max} .

States will be represented as a vector $\mathbf{s} = (\mathbf{s}[1], \mathbf{s}[2], \mathbf{x})$, where \mathbf{x} represents a vector of length $\mathbb{R}^{il_{max}}$. Here, $\mathbf{s}[1]$ signifies the on-hand inventory, $\mathbf{s}[2]$ indicates the total pipeline inventory, and the elements $\mathbf{x}[i]$, $i \in \{1, \dots, \mathbf{s}[2]\}$ with $\mathbf{s}[2] > 0$, denote the elapsed time since the placement of each yet-to-be-received order, while $\mathbf{x}[i] = 0$ for $i > \mathbf{s}[2]$. When $\mathbf{s}[2] = 0$, $\mathbf{x}[i] = 0$, $i \in \{1, \dots, il_{max}\}$. Since we consider a continuous review, continuous time inventory system with several stochastic inputs, i.e., demand and lead times, we employ several strategies to formulate this problem as MDP-EI while staying close to Stolyar and Wang (2022).

We next explain how to construct the exogenous inputs in inventory systems with random lead times and describe the state and the cost transitions. First, we define a (decision) epoch in this system by the duration between two consecutive demands. For each epoch, the exogenous input ξ is depicted as a vector in $\mathbb{R}^{il_{max}+1}$. The element $\xi[il_{max} + 1]$ denotes the interarrival time between the current demand and the next one, i.e., between the current decision epoch and the next. The elements $\xi[i]$, where $i = 1, \dots, il_{max}$, determine for each order in the pipeline (including those orders placed in the current epoch) whether it will arrive before the next epoch and when.

It is sufficient to let $\xi[il_{max} + 1]$ be distributed following the interarrival time of demand, while $\xi[i]$ for $i = 1, \dots, il_{max}$ will be uniformly distributed, regardless of the lead-time distribution. In particular, after placing (zero or more) orders in a decision epoch, ξ is observed, and the state of the system at the beginning of the next epoch can be determined as follows. Consider any order i ($i \in \{1, \dots, \mathbf{s}[2]\}$) that is in the pipeline at the start of the current epoch (after placing orders). It will arrive before the next epoch with probability $p = \mathbf{P}(L \leq \mathbf{x}[i] + \xi[il_{max} + 1] | L > \mathbf{x}[i])$, where we denote by L a generic random variable representing a replenishment lead time. Now, if $\xi[i] \leq p$, then we interpret this as meaning that the order has arrived during the current epoch, and the inventory position $\mathbf{s}[1]$, the pipeline $\mathbf{s}[2]$, and the vector \mathbf{x} are updated accordingly. The value of $\xi[i]$ can also be used to construct the arrival time of the order (between the time associated with the current and next epoch). The arrival times can be used to derive an expression for the cost function $C(\mathbf{s}, a, \xi)$, i.e., the holding costs and backorder costs accrued between the current and the next epoch. (This expression is a bit involved but mostly straightforward and therefore omitted.) If $\xi[i] > p$, the order is still in the pipeline at the start of the next epoch, and $\mathbf{x}[i]$ is updated accordingly. Specifically, when the next epoch starts, the time elapsed since i was placed equals $\mathbf{x}[i] + \xi[il_{max} + 1]$. In the next epoch, it will again be determined whether the order will arrive.

After reviewing each order, the demand is observed, and the holding costs and backorder costs are incurred considering the time between the last incoming order and the demand (or the interarrival time of the demand ($\xi[il_{max} + 1]$) if no order is received). Then the inventory level is decreased by one, and the next epoch starts.

We will use the base-stock policy as the initial policy π_0 . Drawing from the approach detailed by Stolyar and Wang (2022) (see the e-companion for the corresponding calculations), we truncate the infinite state space to apply DCL feasibly, setting specific boundaries for this purpose. Notably, the decision-maker maintains the inventory position within a fixed, finite range. This strategy is reflected in the inequality $I_{min} \leq \mathbf{s}[1] + \mathbf{s}[2] + a \leq I_{max}$, where I_{min} and I_{max} denote the minimum and maximum inventory levels, respectively. We also implement a cap on the maximum number of back-orders, denoted as BO_{max} , and any unsatisfied demand after this limit is lost, incurring the same backorder cost. Consequently, the maximum number of orders that can be in the pipeline inventory can be computed as $il_{max} = I_{max} + BO_{max}$. We note that these boundaries only truncate those states that are less likely to be visited under any policy, allowing us to focus on the more probable and relevant states.